Quaternary Science Reviews 34 (2012) 1–15

Contents lists available at SciVerse ScienceDirect

Quaternary Science Reviews

journal homepage: www.elsevier.com/locate/quascirev

# Tree-ring analysis of ancient baldcypress trees and subfossil wood

David W. Stahle [a,*], Dorian J. Burnette [a,1], Jose Villanueva [b,2], Julian Cerano [b,2], Falko K. Fye [a,1], R. Daniel Griffin [c], Malcolm K. Cleaveland [a,1], Daniel K. Stahle [a,1], Jesse R. Edmondson [a,1], Kathryn P. Wolff [a,1]

[a] Tree-Ring Laboratory, Department of Geosciences, Ozark Hall 113, Fayetteville, AR 72701, USA
[b] Laboratorio de Dendrocronologia, Instituto Nacional de Investigaciones Forestales, Agricolas, y Pecuarias, CENID-RESPID, Km 6.5 margen derecha canal Sacramento, Gomez Palacio, Durango, Mexico
[c] Department of Geography, University of Arizona, Tucson, AZ 85721, USA

ARTICLE INFO

*Article history:*
Received 10 August 2011
Accepted 8 November 2011
Available online 30 January 2012

*Keywords:*
Baldcypress
*Taxodium distichum*
*Taxodium mucronatum*
Dendrochronology
Earlywood
Latewood
ENSO
Subfossil wood

ABSTRACT

Ancient baldcypress trees found in wetland and riverine environments have been used to develop a network of exactly dated annual ring-width chronologies extending from the southeastern United States, across Mexico, and into western Guatemala. These chronologies are sensitive to growing season precipitation in spite of frequently flooded site conditions, and have been used to reconstruct moisture levels the southeastern United States and Mexico for over 1000 years. The El Nino/Southern Oscillation (ENSO) is a major influence on the climate reconstructions derived from these baldcypress chronologies, especially in Mexico where some of the most extreme reconstructed droughts occurred during El Nino events. In the Southeast, the ENSO influence on climate and tree growth changes sign from spring to summer, and this change in dynamical forcing is recorded by sub-seasonal chronologies of earlywood and latewood width. Most existing baldcypress chronologies have been extended with tree-ring data from "subfossil" wood recovered from surface and submerged deposits. Well-preserved subfossil logs have also been recovered in quantity from buried deposits of great age, and may permit development of long continuously dated Holocene chronologies and discontinuous "floating" Pleistocene chronologies. The extensive subfossil baldcypress swamp discovered 6 m below the streets of Washington D.C. was overrun by a transgression of the Potomac estuary, possibly during the previous super interglacial (marine OIS 5e), and provides direct evidence for one potential impact of unmitigated anthropogenic warming and sea level rise.



## 1. Introduction

Baldcypress is a long-lived, deciduous conifer native to the southeastern United States, Mexico, and western Guatemala (Fig. 1). Three species or subspecies have been recognized, including southern swamp baldcypress (*Taxodium distichum*), pond baldcypress (*Taxodium ascendens*), and Montezuma baldcypress (*Taxodium mucronatum*). The species are in the family *Cupressacae*, phylogenetically allied with the sequoias, metasequoia, and a few other subfamilies in Asia. Baldcypress produce clear and anatomically simple annual growth rings that in some cases can be dated to the exact calendar year of formation with dendrochronology (Fig. 2), and several centuries-long ring-width chronologies have been developed from the genus in the southeastern United States, Mexico, and Guatemala (Stahle et al., 1988, 2011a; Stahle and Cleaveland, 1992; Villanueva-Diaz et al., 2007). Precipitation and drought index reconstructions derived from these long cypress chronologies have been used to investigate the dynamics of climate variability over tropical and subtropical North America and to document extreme droughts that may have impacted human activities during the prehistoric and early colonial eras (Stahle and Cleaveland, 1992; Stahle et al., 1998, 2011a, in press; Cook et al., 2007).

Most existing baldcypress chronologies are based on living trees and dead logs from surface, submerged, and partially buried context. Buried subfossil baldcypress wood has been reported widely across the southern United States, including during the 18th century botanical explorations of William Bartram in the lower Mississippi Valley. Recently, hundreds of ancient baldcypress logs have been recovered from deeply buried deposits along the Pee Dee and

* Corresponding author. Tel.: +1 479 575 3703.
*E-mail addresses:* dstahle@uark.edu (D.W. Stahle), djburne@uark.edu (D.J. Burnette), villanueva.jose@inifap.gob.mx (J. Villanueva), cerano.julian@inifap.gob.mx (J. Cerano), ffye@uark.edu (F.K. Fye), dgriffin@email.arizona.edu (R.D. Griffin), mcleavel@uark.edu (M.K. Cleaveland), stahle@uark.edu (D.K. Stahle), jre03@uark.edu (J.R. Edmondson), klp004@uark.edu (K.P. Wolff).
[1] Tel.: +1 479 575 3703.
[2] Tel.: +52 871 719 10 76.

0277-3791/$ – see front matter © 2012 Elsevier Ltd. All rights reserved.
doi:10.1016/j.quascirev.2011.11.005

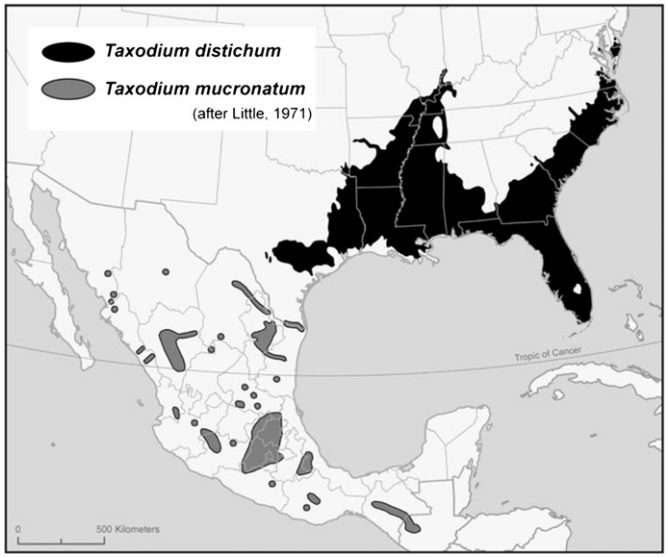


**Fig. 1.** The natural distribution of baldcypress (*T. distichum*) and Montezuma baldcypress (*T. mucronatum*) extends from the southeastern United States, across Mexico, and into western Guatemala (from Little, 1971 and Martinez, 1963). The distribution is highly discontinuous in all areas reflecting the presence of suitable riparian or wetland habitat. The mapping of *T. mucronatum* is incomplete and we have added sites in Sonora, Chihuahua, Tamaulipas, San Luis Potosi, and Oaxaca where we have found the species growing in natural riparian woodlands (smaller dots). The distribution of pond cypress (*T. ascendens*) is more restricted and extends from southeast Virginia to Florida and southeastern Louisiana (not shown).

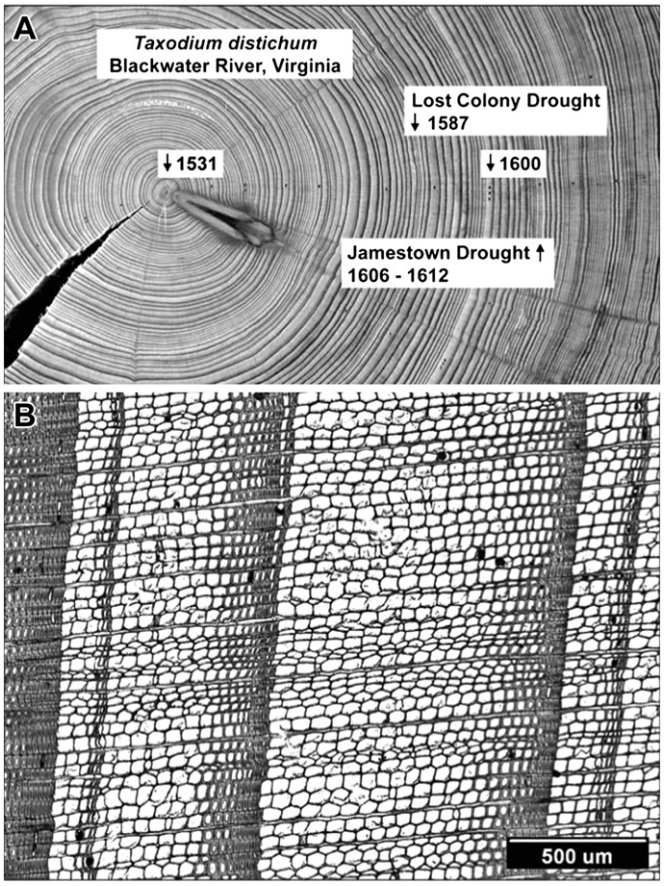


**Fig. 2.** (A) This polished cross-section illustrates the growth rings of baldcypress from Blackwater River, Virginia, including the years of severe drought and narrow tree-rings witnessed during the first English attempts to colonize North America (Stahle et al., 1998). (B) The annual growth rings of *T. distichum* (specimen ID = UWR50) include distinct earlywood and latewood components (light, thin-walled cells vs. darker, thick-walled cells, respectively), which can be used to develop separate chronologies and distinct seasonal climate reconstructions. Note the micro ring that becomes missing towards the bottom of the image.

Lynches Rivers in South Carolina. Subfossil Montezuma baldcypress is much less common in Mexico, but a few submerged specimens have been located in spring pools in San Luis Potosi. The various sources of baldcypress wood from living trees, historic structures, and logs found in surface, submerged, and buried locations offer considerable potential for millennia-long tree-ring chronologies during the late-Holocene, as has been partially achieved in the southeastern United States and at one location in central Mexico (Stahle et al., 1988, 2011a). The massive quantities of well-preserved *Taxodium* wood recovered from subfossil deposits in South Carolina, though unlikely to ever be linked continuously with exactly dated living trees, may allow the development of annual ring-width chronologies for "floating" time intervals during the late Quaternary and would have value for climatic and geochronological research.

This paper reviews the natural history of the genus *Taxodium*, the commercial exploitation of baldcypress timber, and the survival of relict old-growth stands in the United States, Mexico, and Guatemala. The unusual climate response of the derived baldcypress ring-width chronologies is discussed, along with selected applications of these valuable proxy paleoclimatic time series, including the use of earlywood and latewood width chronologies for the development of separate seasonal precipitation reconstructions over the southern United States. We conclude with an overview of the subfossil baldcypress discoveries from the Southeast, their possible origin, and their potential for development of replicated ring-width chronologies for discrete time periods during the Quaternary.

## 2. Natural history

The genus *Taxodium* is recognized in the fossil record from the Mesozoic (>65 million years; Brown and Montz, 1986). During the Miocene (5–24 million years ago) the range of *Taxodium* extended from Eurasia over the Bering Land Bridge and across North America into Mexico and the southern United States (Brown and Montz, 1986; Thomas and Spicer, 1987; Soltis et al., 1992). *Taxodium* was common in the wetlands that formed the widespread deposits of brown coal (Thomas and Spicer, 1987). Global cooling during the Quaternary reduced the range of *Taxodium* to its present distribution in the subtropics of North America (Fig. 1). No species of *Taxodium* survive in natural settings in Eurasia. The relict distribution of *T. mucronatum* in Mexico and Guatemala is highly fragmented and restricted to water courses above 1000 m elevation (Martinez, 1963; Little, 1971; Fig. 1).

The natural history and commercial production of baldcypress was described in "The Southern Cypress" by Mattoon (1915; also see Wharton et al., 1982; Ewel and Odum, 1984; and Brown and Montz, 1986). Mattoon's observations have become particularly valuable because virgin baldcypress forests were heavily exploited and few survive. Mattoon (1915) noted that baldcypress trees in virgin forests of the Southeast routinely reached 35–40 m in height, 2–3 m in diameter above the basal swell, and over 1000 years in age. The largest cypress appear to have been found in South Carolina and Georgia where virgin stands frequently averaged 38 m in height, with individuals 42 m tall scattered through the stand. The finest surviving example of a virgin baldcypress stand with giant columnar trees is the Francis Beidler Forest Sanctuary in Four Holes Swamp, South Carolina, which preserves 710 ha of virgin bottomland hardwood and cypress swamp forests (National Audubon Society, 1985).

Baldcypress is found in four distinct wetland habitats in the southeastern United States (e.g., Wharton et al., 1982), including overflow alluvial swamps along large sediment-rich "brownwater" streams such as the Mississippi, Mobile, Appalachicola, Savanna, and Roanoke Rivers; non-alluvial clear "blackwater" streams fed by springs and seepage that carry very little sediment and are stained dark by the decomposition of organic matter; large near-coastal swamps with slightly brackish tidal water and subject to wind stress and saltwater overflow during heavy gales; and the isolated acidic nutrient-poor ponds found scattered through the yellow pine uplands from Virginia to Florida and Louisiana where the stunted pond cypress (*T. ascendens*) dominates nearly pure stands. Baldcypress appears able to tolerate low levels of salinity, but many near-coastal baldcypress forests have been killed by saltwater intrusion (Allen et al., 1994; Yanosky et al., 1995; Conner and Inabinette, 2005).

Mattoon (1915) made careful studies of the annual growth rings on cypress logs cut from virgin and second growth forests at several locations and concluded that

> "trees from 400 to 600 years old are very common, and those from 600 to 900 years are scattered through most virgin cypress stands."

He noted that the oldest cypress seemed to be found in slightly acid blackwater swamps extending from South Carolina to northern Florida, and believed that the oldest senescent cypress ranged in age from 1000 to 2000 years. Our extensive dendrochronological research on remnant stands of old-growth cypress confirm his observations, although the oldest living baldcypress we have located are in extreme southeastern North Carolina along the Black River where the oldest tree-ring dated individual is at least 1648 years old (Stahle et al., 1988; Early, 1990, and updated to 2011). We have also documented Montezuma baldcypress trees in the 1200- to 1500-year age class at Los Peroles, San Luis Potosi, and at Barranca Amealco, Queretaro (Villanueva-Diaz et al., 2007; Stahle et al., 2011a). Heart rot is prevalent in the oldest remnant cypress stands, so even these dendrochronological results only document minimum tree age. Nonetheless, living baldcypress over 1000-years old are rare and restricted to a few exceptional ancient forests in the United States and Mexico.

In uncut virgin cypress stands, Mattoon (1915) described baldcypress "to be a tree of even-aged groups within all-aged stands," reflecting the infrequent episodic bursts of reproduction only when climatic conditions and swamp water levels became ideal for (a) germination and then (b) several years of rapid height growth to allow the young cypress seedlings to survive subsequent inundations. In some inland swamps on the Atlantic Coastal Plain the age structure of the cypress forest reflected the natural aging and infilling of the water body. Baldcypress trees would form roughly concentric bands of age classes surrounding open water, with the oldest cohort of trees along the upland margin of the swamp and the youngest trees near the center of the lake next to the open water. Mattoon (1915) noted this age structure in particular at Okefenokee Swamp, Georgia, which he illustrated with intricate forest profiles drawn along transects cut through the swamp (Fig. 3A). Moving outward from the "open water" toward higher ground, cohorts of "young cypress," mature cypress in a "pure stand," and "overmature cypress" were often encountered (Fig. 3A), documenting the slow infilling of lakes and the advance of wetland forest onto the accumulating "muck" soils in the size and age of long-lived baldcypress trees. The pure stands of "large cypress" were heavily logged at Okefenokee and across the South, but small stands of decrepit "overmature cypress" (from a forest products perspective) were sometimes left uncut and survive today, representing one fraction of these impressive virgin cypress ecosystems.

He also described the uneven distribution of virgin baldcypress across the subtle topographic surfaces of southern floodplains. The best cypress timber found in the "deep cypress swamp" with the largest clear stems free of branching, was usually found on the organic-rich "muck" soils of backwater swamps away from the main river channels and sloughs (Fig. 3B, far right). Smaller more poorly formed cypress trees were often found along the margins of bayous and sloughs meandering across the floodplain (Fig. 3B, center; also described by Dickeson and Brown, 1848). Some of these "non-commercial," old-growth, streamside baldcypress survived the era of heavy cypress logging and can still occasionally be found lining picturesque Southern waterways.

Our dendrochronological analysis of remnant cypress forests again confirm many of Mattoon's observations on the age structure of living stands, and the descriptions of Dickeson and Brown (1848) on the stratigraphy of cypress logs buried beneath living stands. A crude chronological succession is sometimes evident among living cypress trees and dead wood, including cohorts of young pole-sized trees <100-years old, several cohorts of centuries to millennium-old trees, standing dead trees, fallen logs of various age and decomposition, and partially buried logs. Depending on the recent geological history of the alluvial swamp, we presume that older buried logs and stumps may be roughly stratified beneath some ancient cypress forests, as described for virgin forests by Dickeson and Brown (1848; see Section 7).

This idealized age structure of virgin baldcypress stands has contributed to the development of very long tree-ring chronologies. Using dendrochronology, the unique climate-induced time series

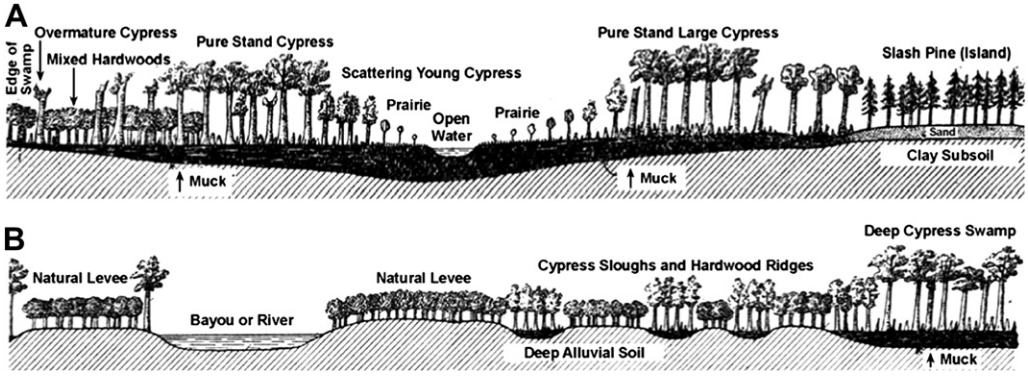


**Fig. 3.** (A) This schematic profile drawn through part of Okefenokee Swamp, Georgia, by Mattoon (1915) illustrates the variable age structure and timber value typically found in virgin cypress stands surrounding open water bodies (left center), and provides a conceptual model for where "overmature" non-commercial cypress-tupelo woodlands can still be found in the southeastern United States. (B) Mattoon's (1915) drawing of the landforms and virgin bottomland forests typical of southern floodplains. This cross-section emphasizes the importance of relatively subtle changes in landforms, soils, and water levels on the size and commercial value of cypress timber in virgin floodplain forests.

patterns of ring widths from living trees, dead trees, fallen logs, and buried logs can be cross-synchronized and placed in their exact calendar year order. In doing so, we have developed several baldcypress tree-ring chronologies in the southeastern United States and Mexico over 1000-years long (Fig. 4). Most of these southeastern chronologies have utilized old living trees and dead wood found on the swamp surface. Subfossil wood is less common in the high-gradient stream habitat of Montezuma baldcypress in Mexico. However, even in the Southeast the scientific exploitation of buried cypress logs has been very limited due to the difficulties in locating and sampling subfossil logs buried in alluvial deposits beneath forested wetlands. For this reason, the recovery of many ancient subfossil cypress logs during the routine sand mining operations at the Pee Dee sand quarries opens the possibility for high resolution analysis of Holocene and late Pleistocene paleoclimate on the Atlantic Coastal Plain.

## 3. Commercial exploitation

The natural range of swamp baldcypress (*T. distichum*) in the United States extends from Delaware to Texas on the Atlantic and Gulf Coastal Plains (Fig. 1), but the regions with the maximum commercial production of cypress lumber were much more restricted. Mattoon (1915) mapped and described the areas of cypress lumber production during the early 20th century. The heaviest cypress production occurred in southern Louisiana, and from southern Georgia across northern Florida, with locally heavy production near the Carolina coast and in the Delta of Arkansas and Mississippi. Estimates in 1914 put the total standing volume of baldcypress in the southeastern United States at not less than 40 billion board feet (94,389,200 $m^3$), and the total cut of cypress in 1913 was over 1.09 billion board feet [2,572,105 $m^3$, not counting lath or shingle mills cutting <50,000 board feet (118 $m^3$); Mattoon, 1915]. The percentages of standing cypress by state in 1914 were 38.9 in Louisiana, 26.5 in Florida, 7.4 in North Carolina, 6.9 in Georgia, 6.4 in South Carolina, 5.5 in Arkansas, 4.7 in Mississippi, 2.2 in Missouri, and <1.0% in Virginia, Alabama, and Texas (Mattoon, 1915).

In pure stands of virgin baldcypress in the best regions of the South, especially Louisiana and Florida, 12,000 to 15,000 board feet per acre (28–35 $m^3$ per 0.4 ha) were typically cut over very large timber holdings. Some select stands of virgin cypress produced 100,000 board feet/acre (235 $m^3$/0.4 ha). The record cut reported by Mattoon (1915) was 127,000 board feet (300 $m^3$) from one exceptional acre (0.4 ha) of columnar cypress trees on the Grand River, Louisiana.

The historical logging of baldcypress in the Southeast produced some impressive volumes, but it was excessive and contributed to the extinction of the ivory-billed woodpecker and the Carolina parakeet (Dennis, 1988). Several large tracts of virgin baldcypress in southern Louisiana were considered for the establishment of a "Cypress Swamp National Monument" in 1939 (King and Cahalane, 1939), including magnificent stands near Lake Pontchartrain, the lower Pearl River, and in the Morganza and Atchafalaya floodways. Unfortunately, the National Monument proposal ultimately failed and these cypress swamplands were subsequently logged.

Only three reasonably large tracts of uncut virgin cypress with large commercially valuable trees have been preserved, none of which are located in Louisiana which by all accounts had the most impressive virgin stands. The National Audubon Society manages two of the finest examples of virgin cypress that remain accessible to the public today, the Francis Beidler Forest Sanctuary in Four Holes Swamp, South Carolina, and the Corkscrew Swamp Sanctuary in southern Florida. A 1200-ha wetland dominated by large baldcypress trees also survives on private property at Grassy Lake, Arkansas. There are smaller stands with giant old-growth cypress still found on public and private land throughout the native range of the species (Fig. 5), but the over-exploitation of the bottomland hardwood/baldcypress forest ecosystem is an example of the failure of public and private conservation in the southeastern United States during the early 20th century.

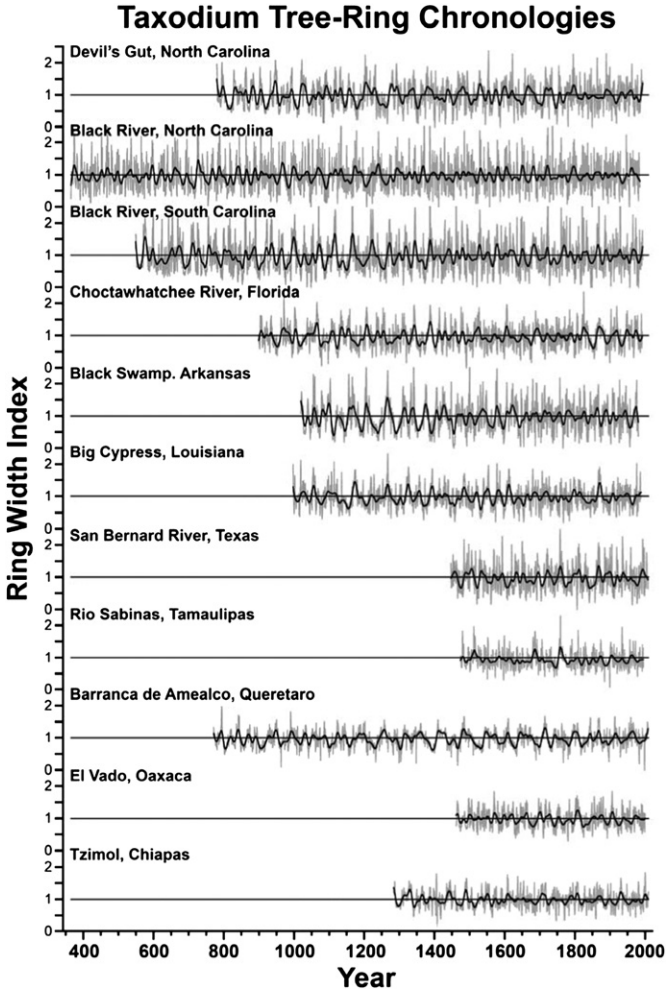


**Fig. 4.** Selected long baldcypress chronologies from the southeastern United States and Mexico (arranged from the Carolinas into southern Mexico, top to bottom). The time series represent detrended and standardized annual values of total ring width (gray) and a smoothed version highlighting 20-year (black). Note the high variance of the chronologies from the Carolinas, and the lower variability typical of the Mexican series.

## 4. A conceptual model for the survival of ancient baldcypress

Baldcypress was found in a variety of native wetland conditions and produced several grades of cypress lumber, some more valuable for timber production than others (e.g., Fig. 3). As a result, small stands of ancient baldcypress trees found in non-commercial forests survived the era of massive timber cutting and agricultural land clearing, and today still contain some of the oldest trees left in eastern North America. Black River, North Carolina, is perhaps the best example of an ancient non-commercial cypress stand that was readily accessible to logging, but was dominated by cypress trees too shaky, pecky, heart-rotten, and "overmature" to justify logging. Today, the Black River site contains the oldest-known living baldcypress trees and some 4450 ha along the river are under conservation management by The Nature Conservancy and the State of North Carolina.

**Fig. 5.** Ancient baldcypress (*T. distichum*) located at Long Lake Slough, Calhoun County, Arkansas (stems are 1–2 m in diameter above the basal swell, photo by Keith Newton). Note the cypress "knees" (right center).

In fact, many Southern sloughs and bayous are still lined with ancient non-commercial cypress trees. These stream or lake-side trees are often poor candidates for saw log production due to their open-grown canopies, massive basal swell, heavy lateral branching, lack of clear stem, and relatively stunted size when grown in the marginal deep-water conditions near open water. The best cypress growth was observed in the broad level backswamps away from the main stream channels where the cypress were obliged to grow up under an unbroken canopy over 30 m high, producing the remarkably dense forests of tall, smooth, columnar cypress stems so excellent and so heavily exploited for lumber production. This environmental gradient in the form and size of ancient cypress trees across virgin southern floodplains was illustrated by Mattoon (1915), and represents a valuable conceptual model for where in the heavily disturbed modern landscape uncut ancient baldcypress can still be found (Fig. 3; Stahle et al., 2006).

The differences between non-commercial and commercially valuable timber was also described and illustrated in the mid-19th century by Dickeson and Brown (1848):

> "In the texture and quality of cypress timber there is a very considerable variety, depending, in a great measure, upon the condition of the localities where it is produced. That growing along the bayous is usually much smaller, more scrubby and of a stunted body, giving out limbs, more or less large, at short distances from the place where the base ceases to swell, all along its body, and enlarging into a wide spreading top. They have but little resemblance to those growing in the basins. A great portion of the cypress timber growing along the sloughs, around the margins of lakes and imperfectly formed basins, is of this description, being coarse, defective, and knotty; affording a very inconsiderable amount fit for market. But the timber growing in the more perfectly formed basins, seems to attain all the perfection of its nature, furnishing the best quality of timber for architectural purposes."

The high quality timber was thoroughly cut across the South, but ancient non-commercial baldcypress survive locally. These are not huge stands and many have suffered selective logging or other human disturbances. But they are representative of one aspect of the original baldcypress forests of the Southeast, the stunted non-commercial variety of exceptionally old trees, and they add beauty and interest to many Southern waterways. Examples of ancient non-commercial baldcypress can be seen at Black River, North Carolina, Choctawhatchee River, Florida, Sky Lake, Mississippi, Bayou DeView, Arkansas, Big Cypress State Park, Louisiana, and the San Bernard River, Texas.

The irregular distribution of Montezuma baldcypress reflects in part the uneven presence of suitable riparian habitat in semi-arid Mexico (Fig. 1). Montezuma baldcypress is the national tree of Mexico and is a protected species (Villanueva-Diaz et al., 2007). Nonetheless, it has been extensively cut for local timber production and has been damaged by agricultural and urban development, water appropriation, and water contamination. An important and only lightly disturbed stand of ancient Montezuma baldcypress survives at Barranca de Amealco, Queretaro (Fig. 6). Several trees at this site are over 1000-years old and with the sparsely scattered ancient cypress at Los Peroles, San Luis Potosi, are the oldest known trees in Mexico. Ancient Montezuma baldcypress trees, some approaching 1000-years in age, are also present along the Rio Nazas in Durango and near Tzimol, Chiapas.

Montezuma baldcypress extends into western Guatemala, but only locally along a few streams. The best Guatemalan baldcypress we have located are on the Rio Lagartero, which runs along and across the international border with Mexico in western Guatemala. We have developed a 500-year long tree-ring chronology from these Guatemalan cypress, but a few of the oldest trees at Rio Lagartero are likely over 800-years old.

## 5. The climate response of baldcypress tree-ring chronologies

A network of centuries to millennium-long baldcypress tree-ring chronologies has been developed from living trees and subfossil wood in the United States, Mexico, and Guatemala (Fig. 7). Eleven selected baldcypress chronologies are illustrated in Fig. 4. These total ring-width series were all detrended and standardized identically and are plotted on the same scale to highlight differences in the absolute variance among the chronologies [i.e., all component series were detrended using a smoothing spline with 50% frequency response of 100 years, with robust estimation of the mean value function, and by detrending the variance of the robust mean chronology with a 100-year spline to minimize variance changes due to declining sample size (using the ARSTAN program; Cook, 1985)]. Note the high interannual and decadal variability of the baldcypress chronologies from the Carolinas (Fig. 4), which are strongly correlated with precipitation and the soil moisture balance during the spring-early summer season (e.g., Stahle et al., 1988; Stahle and

**Fig. 6.** Ancient Montezuma baldcypress (*T. mucronatum*) trees on a tributary of the Rio San Vicente near Tzimol, Chiapas. These trees are 1–3 m in diameter, 30 m tall, and range from 200- to over 800-years old.

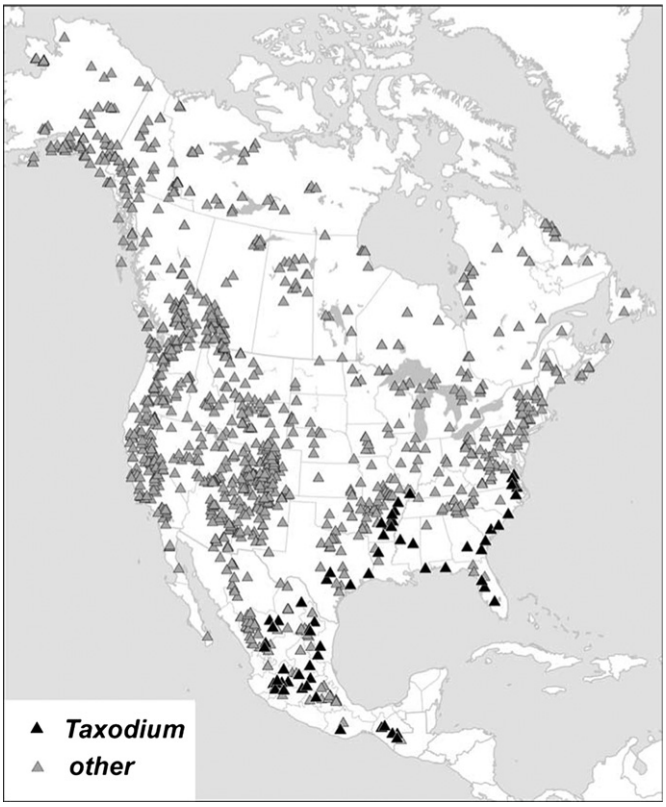


**Fig. 7.** The network of North American tree-ring chronologies is illustrated, all derived from old-growth forests with trees at least 200-years old and many with trees over 500-years old. Most of these chronologies are sensitive to precipitation and have been used as proxies for the reconstruction of past drought and wet years (e.g., Cook et al., 2007). The chronologies developed from baldcypress trees are located with black triangles, and were obtained from forested wetlands that include the oldest-known trees in the eastern United States and Mexico.

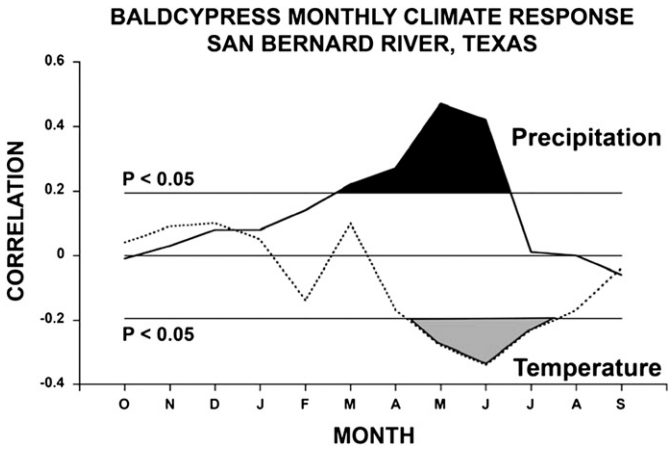


**Fig. 8.** The climate response of an annual ring-width chronology of baldcypress from the San Bernard River, Texas (Fig. 4), is illustrated for the water year (including months preceding, concurrent with, and following the growing season). Note the significant positive correlations with monthly precipitation and negative correlations with temperature during the growing season (March–July). This is the same climate response typical of upland trees on dry sites, but has been observed for baldcypress chronologies throughout its native range in spite of frequently flooded site conditions. The monthly precipitation and temperature data were obtained for Texas climate division 8 (http://www.esrl.noaa.gov/psd/data/usclimdivs/).

Cleaveland, 1992). The interannual variability of the *T. mucronatum* chronologies from Mexico is uniformly lower than the variability in the *T. distichum* chronologies from the U.S. (Fig. 4), but many of these Mexican baldcypress chronologies nevertheless have a very strong climate signal (e.g., Stahle et al., in press). The two longest baldcypress chronologies currently available were developed at Black River, NC, and the separate Black River, SC (Fig. 4). Both sites include exceptionally old living trees, especially at Black River, NC, which contains extensive stand with some of the oldest living trees ever reported for eastern North America. The tract of ancient baldcypress at Black River, NC, is surely one of the most remarkable natural areas left in the southern United States (Stahle et al., 2011b).

Baldcypress chronologies are excellent proxies of the growing season moisture balance, in spite of the frequently flooded natural habitat. In fact, baldcypress is one of the few native tree species that can tolerate such frequently flooded conditions (e.g., Wharton et al., 1982), which outwardly appear to contradict one of the basic principles of tree-ring dating, the concept of site selection. The strongest climate signal in arid-site conifers is often found in trees from steep sunny slopes where soil moisture is supplied only by precipitation (Douglass, 1920; Stokes and Smiley, 1996; Fritts, 2001). However, in every baldcypress chronology reported thus far, ring-width growth is directly correlated with precipitation and inversely with temperature during the growing season (e.g., Fig. 8), the classic climate response of upland trees on moisture-limited sites. Many cypress sites experience huge fluctuations in seasonal and interannual water levels due to natural climate variability, and this is part of the explanation for the climate response of the species. But the stratification of dissolved oxygen (DO) that tends to develop in the swamp and soil water in these southern wetlands also appears to render baldcypress trees particularly sensitive to water levels changes (Stahle and Cleaveland, 1992). High water temperatures and high biological oxygen demand during the growing season can lead to anoxic conditions at depth, which tend to impede the penetration of the fine root systems of baldcypress. These perched feeder root systems are obvious at many native baldcypress stands in the United States and Mexico during low water conditions, and they render the plant vulnerable to internal moisture stress with only relatively minor fluctuations in water level. The seasonal climate response of baldcypress total ring-width chronologies is largely restricted to the first half of the growing season, generally March to July (e.g., Fig. 8). We presume that the absence of monthly precipitation or temperature response before March is due to cool season dormancy and the lack of response after July likely reflects high evapotranspiration demand, lower water quality (especially reduced DO), and the hazard of internal moisture stress.

The correlation between cypress radial growth and rainfall is fairly consistent for all levels of precipitation, not just below average conditions. Apparently, these trees benefit from improved water quality during above average precipitation conditions (presumably both in terms of dissolved oxygen and available nutrients; Stahle and Cleaveland, 1992). Experimental support for this interpretation of the baldcypress growth response was reported by Davidson et al. (2006) based on pieziometer studies, who found increased growth rates during high precipitation events when the moisture flux through the root system was high, along with dissolved oxygen and nutrient levels.

Baldcypress ring-width chronologies are dominated by high interannual to decadal variability, and do not tend to preserve century scale fluctuations in growth that might be linked with low-frequency climate changes. The mean ring-width time series for this species tend to be highly non-stationary in the mean and variance, so each measured radius is detrended and standardized with empirical curve fitting techniques to remove effects of the mean in the computation of the average chronology and to minimize low-frequency changes arising from the biological effects of increasing tree age and size (Fritts, 2001). Unfortunately, any low-frequency

climate changes embedded in the raw ring-width data will also tend to be removed upon detrending and standardization. This is a fundamental limitation that may impact all tree-ring data for which there is no universal solution (Cook et al., 1995). Alternative standardization techniques have been developed that can maximize low-frequency variability in the derived chronologies (so-called "regional curve" and "signal free" standardization, Briffa and Melvin, 2011). But the unique frequently flooded environment and physiological response of baldcypress trees appear to create a kind of "natural high pass filter" that allows the trees to adapt to centennial-scale changes in mean water level. Baldcypress trees can adventitiously sprout fine root systems from the stem, upper root system, and "knees" (vertical root formations, sometimes over 1–2 m tall; Fig. 5) to track long-term changes in mean water levels and to maximize the fine feeder root mass in the zone of well-oxygenated near surface water. If the mean water level is lowered for decades, then baldcypress seem able to sprout new rootlets at lower levels on the stem, lateral roots, and knees to continue to supply moisture and nutrients to the plant. Or conversely they can abandon low-level fine roots and sprout new roots higher up the stem and knees when the water level is persistently raised. In fact, the most important physiological function of knees, which has been long debated (Kurz and Demaree, 1934), may be to increase the fine root mass in the zone of well-oxygenated near surface water, more than would be possible solely with roots skirting the main stem.

This physiological mechanism is illustrated at Reelfoot Lake, TN, which was created by the New Madrid earthquakes of 1811–1812 and the streamside cypress were permanently inundated to a depth of 2 m (Stahle and Cleaveland, 1992; Stahle et al., 1992). The Reelfoot Lake baldcypress that survived the inundation sprouted a new root system nearly 2 m up the stem in the well-oxygenated near surface waters (the so-called hanging buttresses of Reelfoot Lake, Kurz and Demaree, 1934). This "root system tracking" of long-term changes in mean water level appears to be a physiological response of baldcypress to the strong down water gradient in DO during the growing season. Baldcypress appears to be particularly capable of root system tracking of long-term changes in moisture levels because of its natural stream margin habitat, but some plasticity in the long-term climatic response probably exists for most tree species, which may degrade the registration of low-frequency climate change regardless of the methods used for chronology development.

## 6. Discrete seasonal precipitation reconstructions from baldcypress earlywood and latewood width

### 6.1. Climate response of earlywood and latewood width

Baldcypress trees form a prominent latewood band, particularly at *T. distichum* sites in the Southeast. In those circumstances it is possible to use simple measuring protocols to develop separate earlywood (EW) and latewood (LW) width chronologies to further subdivide the seasonal climate signal in the radial growth of these ancient trees (e.g., Stahle et al., 2009). The spatial correlation of the climate signal in an average EW width chronology developed from baldcypress trees on the Altamaha River, Georgia, and the Choctawhatchee River, Florida, is illustrated in Fig. 9A, using the 0.5° grid of instrumental monthly precipitation developed by R.R. Heim, Jr., of NOAA's National Climatic Data Center (personal communication; Stahle et al., 2011a, in press). The strongest precipitation correlations with EW were observed for April and May, centered over Georgia (Fig. 9A).

Because EW and LW widths are measured on subannual components of the same rings from the same trees, there tends to be a strong intercorrelation between EW and LW width chronologies. And

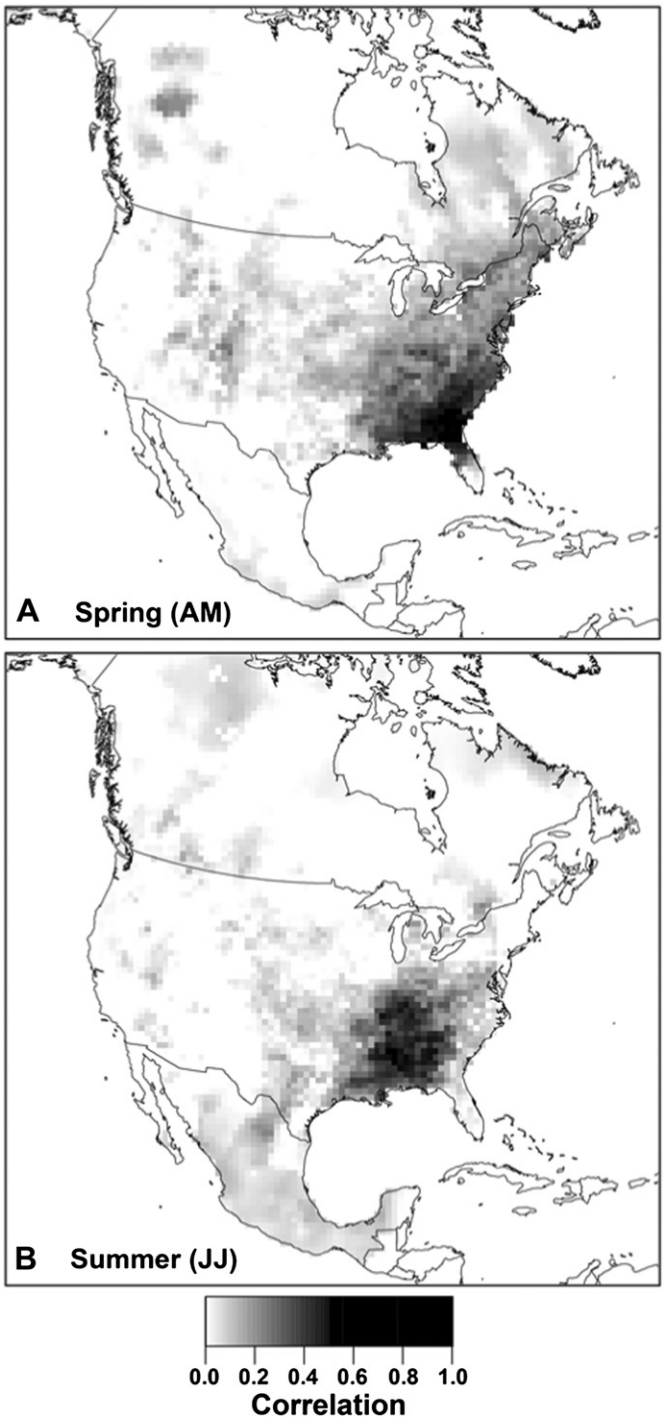


**Fig. 9.** The spatial distribution of the precipitation correlation with baldcypress EW (A) And LW (B) chronologies from the Southeast is mapped (based on an average of the residual chronologies from the Altamaha and Choctawhatchee Rivers). The EW chronology was correlated with spring (AM) precipitation totals at each grid point, the adjusted LW chronology with summer (JJ) precipitation totals at each point (only positive correlations are mapped). The Southeastern grid points exhibiting strong correlation with EW and LW were extracted and used to compute the regional average instrumental spring (A) and summer (JJ) precipitation series. For spring, 72 grid points were extracted from central Alabama to the Georgia coast, and 56 points from Alabama into central Georgia were used to compute the summer series (Fig. 10; grid points listed at http://www.uark.edu/dendro/baldcypress/qsr.xls).

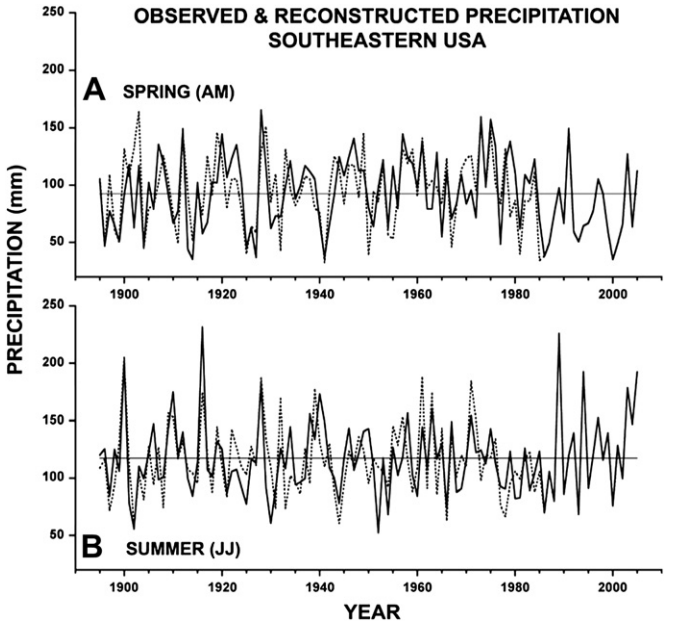


**Fig. 10.** The observed (solid lines) and reconstructed spring (AM) and summer (JJ) precipitation series (dashed lines) for the southeastern United States are plotted from 1895 to 1985 (A and B, respectively). The instrumental series are also plotted from 1986 to 2005 to update the reconstructions. Note the dryness in spring and wetness in summer after 1985. The spring and summer precipitation series are not correlated for either the instrumental or reconstructed data, and the modest but statistically significant ENSO signal detected in these reconstructed precipitation data changes sign from spring to summer (Fig. 12).

because the seasonal climate variables to which these subannual ring-width chronologies respond do not tend to be intercorrelated, we attribute the intercorrelation to physiological persistence within the sample trees and remove the dependency of LW on EW width statistically. The LW width chronology was regressed on the EW chronology for both the Altamaha and Choctawhatchee River collections, and the residuals from regression were used to estimate the pure LW variability independent of the variation in EW width at each site (i.e., the so-called adjusted LW chronology, $LW_{adj.}$, Meko and Baisan, 2001; Stahle et al., 2009). The regional and seasonal climate response of the adjusted LW width chronology averaged for the Altamaha and Choctawhatchee Rivers is illustrated in Fig. 9B.

The Kalman filter (Visser and Molenaar, 1988) can also be used to cleanse the LW chronology of its dependency on EW, and may be particularly useful when there is a strong time dependency in the relationship (E.R. Cook, personal communication). We conducted a series of experiments to remove the EW signal from LW on both an individual tree-by-tree basis and on the mean index chronologies, using both linear regression and Kalman filter techniques. For the baldcypress chronologies we investigated, the best results were achieved by taking the residuals from regression of the LW mean index chronology regressed on the EW chronology, where "best" is here defined as an adjusted LW chronology with the strongest response to warm season precipitation and moisture balance indices.

The adjusted LW chronology average from the Altamaha and Choctawhatchee Rivers is most strongly correlated with June–July average precipitation over Alabama and adjacent states (Fig. 9B). The LW correlation with JJ precipitation is shifted westward compared with the EW correlation with AM precipitation, but the spatial signals overlap in western Georgia and eastern Alabama (Fig. 9A,B). However, the seasonal climate signals do not overlap, such that the EW chronology is not correlated with summer climate, and the LW chronology is not correlated with spring climate. Consequently, these partial ring chronologies provide separate seasonal climate information for the southeastern United States over the past 1000 years.

### 6.2. Reconstruction methodology

To reconstruct spring precipitation over the Southeast, the seasonalized April–May precipitation totals were first extracted from the Heim 0.5° grid (Fig. 9A) and averaged into a spring instrumental regional average for calibration with the EW tree-ring data. Instrumental June–July precipitation totals at each grid point were extracted from the region illustrated in Fig. 9B, and then averaged into a single regional time series for calibration with the LW chronology data. The extraction region for spring was centered on Georgia, and on Alabama for summer, but both include the drainage basins of the Chattahoochee, Flint, and Apalachicola Rivers, which supply water to metropolitan Atlanta and were seriously impacted during the severe two-year drought from 2005 to 2007 (Seager et al., 2009).

Standard EW and adjusted LW width chronologies from the Altamaha and Choctawhatchee Rivers were used for the reconstruction of Southeastern spring (AM) and summer (JJ) precipitation, respectively. To compile the standard chronologies, the EW width series for each radius were detrended by fitting a cubic smoothing spline to the EW measurements and then computing the indices as the ratio of the fitted detrending curve in year $t$ to the EW width value also in year $t$. The EW indices for each radius were then used to compute the mean index EW standard chronology, using robust estimation of the mean to discount outliers (Cook, 1985). A smoothing spline with a fixed frequency response was fit to all EW width series, in this case a spline with a 50% frequency response equal to 100 years (Cook and Peters, 1981). This 100-yr frequency response defines a spline function that is sufficiently flexible to provide good detrending of the raw EW growth values, which are subject to substantial and persistent changes in mean and variance, while not attenuating the large decadal excursions in growth which are coherent among tree-ring collection sites in the Southeast and appear to reflect regional climate variability. The same 100-yr frequency response was used to define spline detrending and indexing curves for the LW widths, and the LW chronology was also computed as the robust mean of the indices available in each year.

The standard EW chronologies for Altamaha and Choctawhatchee, including two lead and two lagged versions of each chronology (i.e., for years $t_{-2}$, $t_{-1}$, $t_0$, $t_{+1}$, $t_{+2}$), were entered into forward stepwise multiple regression as potential predictors of April–May precipitation totals in year $t$ for the Southeast (the predictand). The predictor and predictand variables were first submitted to autoregressive (AR) modeling and only persistence-free variables [AR(0)] were passed to regression (AR model order selected with the Akaike Information Criteria, AIC, Cook et al., 1999). The Altamaha and Choctawhatchee EW chronologies in year $t$ were both selected as significant predictors of AM precipitation ($P < 0.05$), but no lagged variables were selected. The transfer function used to estimate AM precipitation from the EW tree-ring chronologies was:

$$\hat{Y}_t = 0.002 + 1.283X_{1_t} + 1.03X_{2_t} \quad (1)$$

The coefficients of this transfer function were derived from the regression model, where $\hat{Y}_t$ is the estimate of AM precipitation totals in year $t$ for the southeastern United States region described in Fig. 9A, $X_{1_t}$ is the standard EW width chronology from the Altamaha River in year $t$, and $X_{2_t}$ is the standard EW width chronology from the Choctawhatchee River also in year $t$. This regression model represents 41% of the variance in April–May precipitation for the 1895–1985 calibration period ($R^2_{adj} = 0.41$; Table 1). Split period calibration and verification experiments indicate that this regression model is stable during subperiods of the 20th century (Table 1).

**Table 1**
Calibration and verification statistics for the reconstruction of spring (AM) and summer (JJ) precipitation over the southeastern United States using EW and LW width chronologies of baldcypress, respectively. The autoregressive time series structure of the predictor and predictands are listed under AR (order n) [column two = predictand, column three = first predictor (indicated in column $b_1$ under Coefficients), column four = second predictor $b_2$ under coefficients]. The predictors used with each coefficient are indicated by letter (A = Altamaha River, C = Choctawhatchee River). Other column headings are $N$ = sample size; $R^2_{adj}$ = coefficient of determination adjusted downward for the loss of degrees of freedom; SE = standard error of the regression estimates; DW = the Durbin Watson statistic [DW = 2.0 desired, no significant autocorrelation of the regression residuals ($P < 0.05$) was found with any model]; $r$ = Pearson correlation coefficient comparing reconstructed with instrumental precipitation data in the alternate statistically independent verification period; the reduction of error (RE) and coefficient of efficiency (CE) statistics were calculated on observed and reconstructed data in the verification period, and both tests indicate successful verification (e.g., the RE approximates $R^2$ during the verification period).

| Time period | AR ($n$) | | | Coefficients | | | $N$ | $R^2_{adj}$ | SE | DW | $r$ | RE | CE |
|---|---|---|---|---|---|---|---|---|---|---|---|---|---|
| | | | | $b_0$ | $b_1$ | $b_2$ | | | | | | | |
| *April–May* | | | | | | | | | | | | | |
| 1895–1944 | 0 | 0 | 1 | 0.000 | 1.355 A | 1.026 C | 50 | 0.42 | 0.962 | 1.89 | 0.64 | 0.40 | 0.25 |
| 1945–1985 | 0 | 0 | 1 | 0.004 | 1.291 A | 0.781 C | 41 | 0.38 | 0.889 | 2.19 | 0.67 | 0.42 | 0.31 |
| 1895–1985 | 0 | 0 | 1 | 0.002 | 1.283 A | 1.030 C | 91 | 0.41 | 0.942 | 1.90 | | | |
| *June–July* | | | | | | | | | | | | | |
| 1895–1944 | 0 | 0 | 0 | 0.000 | 2.132 C | 0.690 A | 50 | 0.42 | 1.025 | 2.26 | 0.56 | 0.27 | 0.26 |
| 1945–1985 | 0 | 2 | 0 | −0.001 | 0.975 A | 1.048 C | 41 | 0.30 | 0.839 | 2.17 | 0.62 | 0.35 | 0.34 |
| 1895–1985 | 0 | 0 | 0 | 0.000 | 1.804 C | 0.735 A | 91 | 0.39 | 0.941 | 2.13 | | | |

The regression results for calibrations based on the 1895–1944 and 1945–1985 subperiods are included in Table 1, along with selected verification statistics for the alternate statistically independent validation intervals (i.e., 1945–1985 and 1895–1944, respectively). The explained variance ranges from 0.38 to 0.42 for these two shorter calibration periods and both verify on independent spring precipitation data.

Equation (1) was used to estimate AM precipitation from AD 929–1985 and the persistence structure observed in the predictand during the calibration period was added into the reconstructed estimates [in this case only the intercept term of the AR(0) model, Table 1]. The variance lost in regression, computed as the ratio of standard deviations between the observed and reconstructed series during the calibration period (1895–1985), was then multiplied through the reconstruction so that the instrumental AM precipitation totals from 1986 to 2005 (the end year of the Heim dataset) could be appended to the outer year of the reconstruction and thus complete the reconstruction and updated time series from AD 929–2005 (Fig. 11A).

The standard LW chronologies from Altamaha and Choctawhatchee, also including two lead and two lagged versions for each site, were entered into forward stepwise regression with June–July precipitation totals over the Southeast (i.e., for years $t_{-2}$, $t_{-1}$, $t_0$, $t_{+1}$, $t_{+2}$). The same procedures described for the reconstruction of AM precipitation from the EW chronologies were used for the LW estimation of JJ precipitation. The transfer function used to estimate JJ precipitation was:

$$\hat{Y}_t = 0.00 + 1.804X_{1_t} + 0.735X_{2_t} \quad (2)$$

where $\hat{Y}_t$ is the estimate of JJ precipitation totals in year $t$ for the southeastern United States (see Fig. 9B), $X_{1_t}$ is the standard LW width chronology from the Choctawhatchee River in year $t$, and $X_{2_t}$ is the standard LW width chronology from the Altamaha River in year $t$. This reconstruction explains 39% of the variance in JJ precipitation for the full 1895–1985 calibration period, and statistical validation experiments demonstrate stability in this model during two subperiods of the 20th century (Table 1). The AR structure of the predictand was used to modify the reconstruction [again using only the intercept term on the AR(0) model], and the reconstruction was rescaled by the ratios of observed and reconstructed standard deviations to restore variance lost in regression. The instrumental JJ precipitation totals after 1985 were appended to the reconstruction, resulting a reconstructed and updated time series of June–July precipitation extending from AD 929–2005 (Fig. 11B).

### 6.3. Analysis of the seasonal precipitation reconstructions

The spring and summer precipitation reconstructions for the southeastern United States are illustrated in Fig. 11A,B along with a smoothed version highlighting decadal variability [i.e., a cubic smoothing spline with a 50% frequency response of 10 years was fit to each reconstruction (Cook and Peters, 1981)]. Both reconstructions cover the period AD 929–1985 and have been updated to 2005 with the instrumental observations for a total of 1077 years. The 20-year period from 1985 to 2004 was the second driest April–May episode in the entire reconstruction, second only to the period from 1179 to 1199 when 23 out of 24 years are estimated to have been below average. This recent spring dryness reverses the modest spring (MAM) wetness trend that prevailed over the Southeast during much of the 20th century (Folland and Karl, 2001; and Fig. 9A).

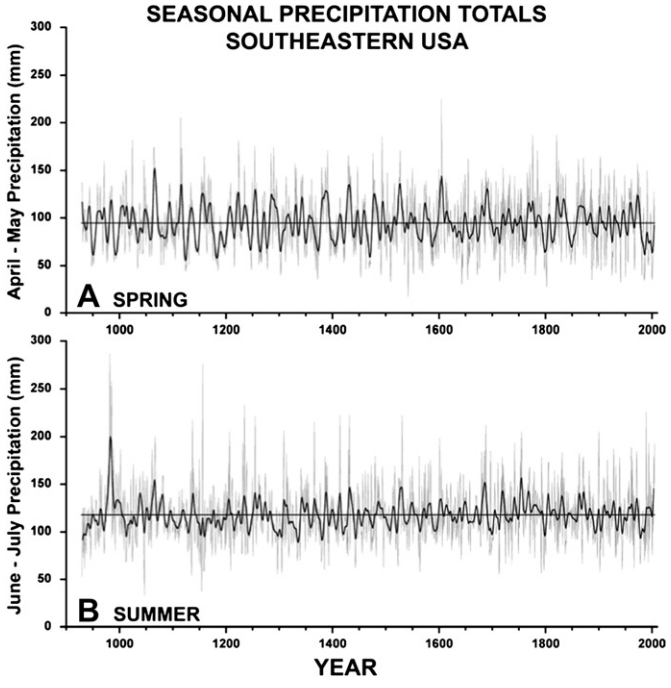


**Fig. 11.** The (A) spring (AM) and (B) Summer (JJ) precipitation reconstructions (gray) for the southeastern United States regions extracted from Fig. 9A,B. Both reconstructions include a smoothed version to highlight decadal variability (black).

Summer (JJ) precipitation was also well below average during the mid-1980s, but shifted to above average conditions from 1989 to 2005 (Figs. 10B and 11B), reversing a modest aridity trend in summer (JJA) precipitation over Georgia during the 20th century (Folland and Karl, 2001). In fact, the spring and summer reconstructions are not correlated at the interannual time scale ($r = 0.10$), and are only weakly correlated at decadal time scales ($r = 0.24$ and 0.15 for 10- and 20-yr spline versions, respectively). Not only are the two reconstructions largely uncorrelated, they appear to exhibit the opposite response to large-scale ocean-atmospheric forcing. Composite and correlation analyses during the instrumental era indicate major differences in the instrumental and reconstructed seasonal precipitation response to El Nino conditions (Fig. 12). The 10 wettest springs and the 10 driest summers reconstructed over the Southeast are both linked with El Nino conditions in the eastern equatorial Pacific, highlighting their contrasting response (Fig. 12A,B; La Nina conditions weakly favor the opposite pattern of dry springs and wet summers over the Southeast, not shown).

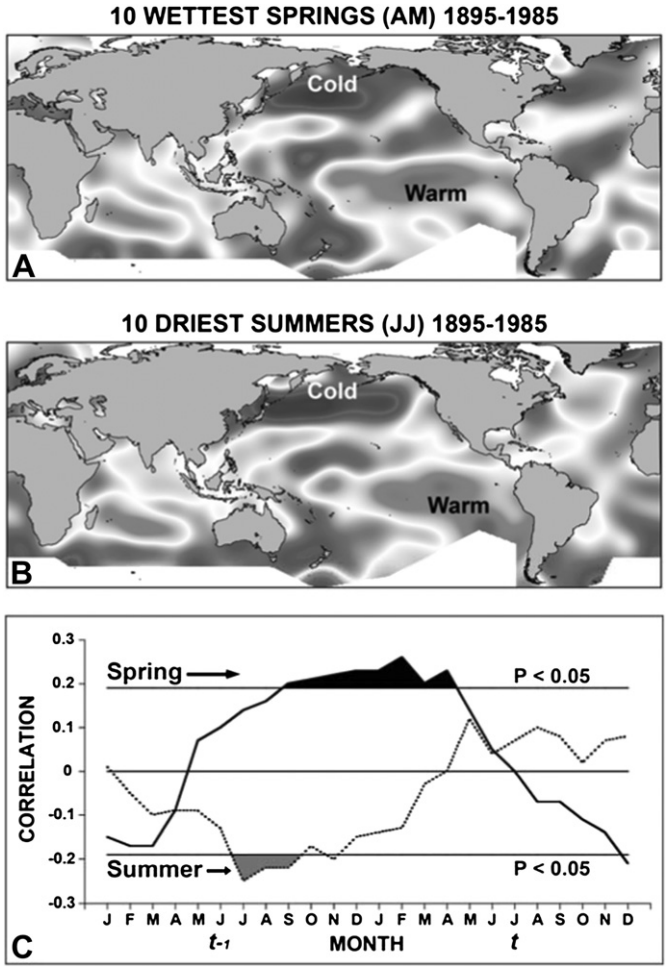


**Fig. 12.** (A) Composite maps of seasonal SSTs (DJFMAM) during the 10 wettest springs and the (B) 10 driest summers reconstructed for the southeastern United States from 1895 to 1985 (the coldest and warmest SST anomalies are labeled; data from Kaplan et al., 1997). ENSO forcing of Southeast precipitation changes sign from spring to summer. Wet springs and dry summers are associated with similar SST anomalies in the Pacific, notably including warm El Nino-like conditions in the eastern tropical Pacific. Dry spring and wet summer conditions are linked with largely the opposite La Nina-like SST patterns in the Pacific, but the anomalies are not strong (not shown). (C) The monthly Nino 3.4 SST index (Rayner et al., 2003) is correlated with the spring (AM) and summer (JJ) precipitation reconstructions for the southeastern United States during the year prior to ($t_{-1}$) and concurrent with ($t$) baldcypress growth and reconstructed precipitation (1881–1985). Note the significant positive correlations between the Nino 3.4 index and reconstructed spring precipitation, and the negative correlations with summer precipitation.

This change in ENSO forcing of seasonal precipitation over the Southeast is apparent when the spring and summer precipitation reconstructions are correlated with monthly ENSO indices (Fig. 12C). The spring precipitation reconstruction is significantly and persistently correlated with Nino 3.4 SSTs during the preceding fall, winter, and early spring. The summer precipitation reconstruction is negatively correlated with the Nino 3.4 SSTs during the preceding summer, fall, and early winter (Fig. 12C). This change in sign may reflect, in part, the tendency for the ENSO system to change phase during the May–June season (Philander, 1990).

These changes in ENSO forcing of spring and summer precipitation over the Southeast justify separate reconstructions of each season using the EW and LW chronologies. In fact, the opposite response to ENSO forcing from spring to summer might also be used to enhance the ENSO signal in the proxy tree-ring data from the Southeast. For example, the Pearson and Spearman correlation coefficients computed for instrumental and reconstructed precipitation over the Southeast and an ENSO index are tabulated in Table 2. The Nino 1.2 index seasonalized for the preceding May–June–July (MJJ) is positively correlated with spring and negatively correlated with summer precipitation for both the instrumental and especially the reconstructed data. When the normalized spring and summer precipitation series are differenced to highlight opposite extremes (e.g., wet spring followed by dry summer, which both seem to be enhanced by El Nino events, Fig. 12A,B), the correlations with ENSO are enhanced for both the instrumental and reconstructed data (Table 2). The stronger ENSO correlations computed for the reconstructed as opposed to the instrumental precipitation series (Table 2) may indicate that the seasonal reconstructions still retain some temperature variability even though they were calibrated solely with precipitation (note that ENSO can influence both precipitation and temperature over the Southeast). Nevertheless, the reconstructed precipitation data for the Southeast are significantly correlated with ENSO ($r = 0.48$; $P < 0.001$; for the normalized difference series, 1931–1985; Table 2), which is the highest ENSO correlation we have yet computed for baldcypress tree-ring data in the southeastern United States (e.g., Stahle et al., 1998) and strong enough to be potentially useful for multi-proxy reconstructions of ENSO variability (e.g., Mann et al., 2000; McGregor et al., 2010) and/or for mapping the response of regional climates to pre-instrumental ENSO regimes identified with other proxies (e.g., Cobb et al., 2003).

It is not possible to derive EW and LW width measurements at all baldcypress sites, particularly with *T. mucronatum* in Mexico, which tends to form very narrow latewood bands often consisting of only one or two cells. However, the ENSO forcing of seasonal climate variability is often very strong in Mexico and tends to have a stronger influence on the growth of Montezuma baldcypress trees. We have

**Table 2**
Correlations between the Nino 1.2 SST index (Rayner et al., 2003) and spring and summer precipitation over the southeastern United States are listed for the 1931–1985 period. Instrumental and reconstructed precipitation totals for spring (AM) and summer (JJ) are compared, along with the normalized difference between AM and JJ totals (to emphasize opposite extremes such as wet springs followed by dry summers). The Nino 1.2 SSTs have been averaged for preceding summer season (MJJ).

| | April–May ppt | June–July ppt | Norm Diff AM–JJ |
|---|---|---|---|
| *Instrumental Precipitation* | | | |
| Pearson $r$ | 0.18 (ns) | −0.21 (ns) | 0.29 (<0.05) |
| Spearman $r$ | 0.18 (ns) | −0.24 (<0.10) | 0.33 (<0.02) |
| *Reconstructed Precipitation* | | | |
| Pearson $r$ | 0.27 (<0.05) | −0.42 (<0.01) | 0.48 (<0.001) |
| Spearman $r$ | 0.20 (ns) | −0.41 (<0.01) | 0.46 (<0.001) |

developed a 1238-year long reconstruction of June PDSI for central Mexico using annual ring widths of Montezuma baldcypress trees in Queretaro (Fig. 13; Stahle et al., in press). This reconstruction is well correlated with ENSO (Fig. 14), and some of the most extreme droughts of the past millennium occurred during strong El Nino years (e.g., 1983, 1998). The correlations between SST in the eastern equatorial Pacific, warm season precipitation and baldcypress growth in central Mexico are negative (Fig. 14), so that El Nino regimes favor drought and low growth. This is generally the opposite of the ENSO forcing to climate and tree growth in the southern United States and northern Mexico, where El Nino conditions favor above average winter-spring precipitation. With this diverse ENSO forcing of climate and baldcypress growth, it should be possible to use EW, LW, total ring width, and potentially density chronologies of baldcypress in the southeastern United States and Mexico for improved reconstructions of past ENSO variability.

## 7. Subfossil baldcypress wood from the southeastern United States and Mexico

Baldcypress is known as the "wood everlasting" and non-lithified "subfossil" logs have been recovered from buried deposits of great antiquity. If enough wood can be recovered from subfossil deposits, then it should be possible to develop crossdated floating chronologies extending back into the Holocene, and perhaps the Pleistocene. The more recent floating segments might eventually be linked with the longest calendar-dated chronologies based on living trees. In fact, many long cypress chronologies have already been extended with relict wood found on the swamp surface, so further extension only requires recovery of older subfossil wood in sufficient quantity to establish replicate crossdating.

Subfossil baldcypress deposits were first described in the late 18th century by the famous pioneer botanist William Bartram. Bartram (1791) described a buried cypress forest exposed at the base of a 30 m river bank on the Mississippi River near Port Hudson, Louisiana, in 1777:

> "here in the cliffs we see vast stumps of cypress and other trees….These stumps are sound, stand upright, and seem to be rotted off about two or three feet above the spread of their roots; their trunks, limbs, &c., lie in all directions about them."

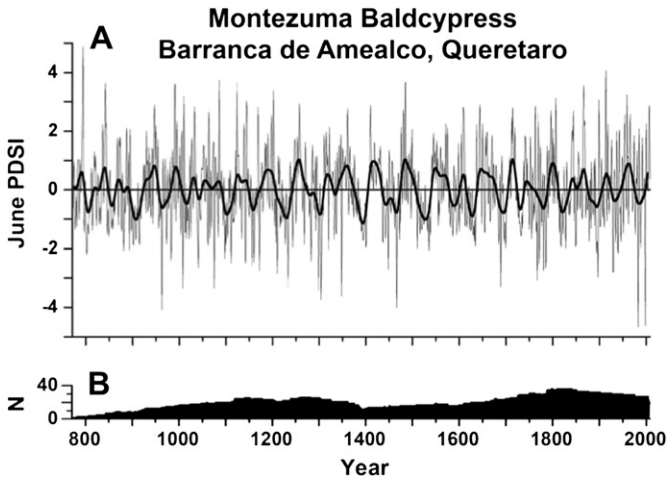


**Fig. 13.** (A) The June PDSI reconstruction for central Mexico derived from the Montezuma baldcypress trees at Barranca de Amealco, Queretaro (from Stahle et al., 2011a). The smoothed time series highlights 30-year departures in reconstructed PDSI. The number of dated radii included in the tree-ring chronology used to estimate June PDSI is plotted below (B).

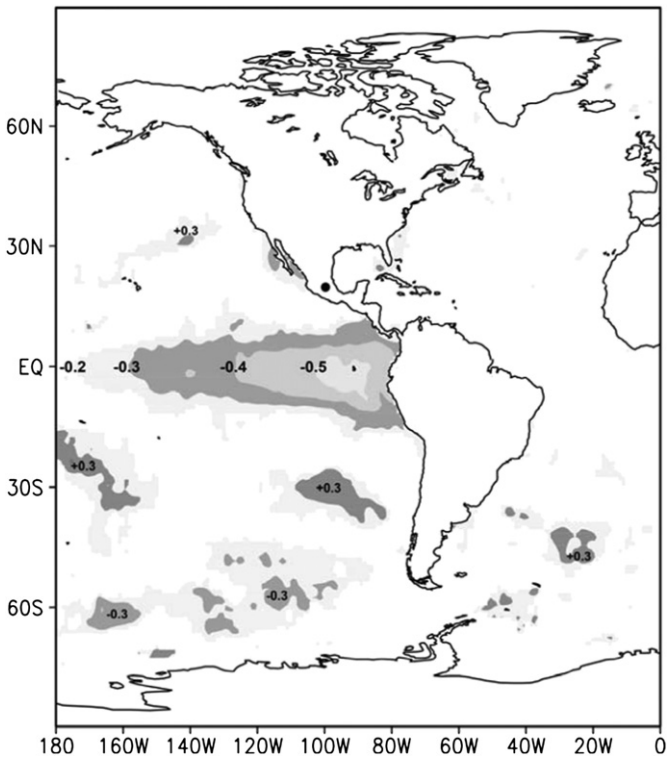


**Fig. 14.** The June PDSI reconstruction for Mesoamerica (black dot) was correlated with gridded SSTs for the boreal winter-spring season (DJFMAM) from 1931 to 2003 [using the KNMI Climate Explorer, only significant correlations ($P < 0.10$) are mapped; http://climexp.knmi.nl/start.cgi?someone@somewhere]. Note the significant negative correlations in the eastern equatorial Pacific, meaning that warm El Nino conditions favor drought over Mesoamerica, the opposite of the El Nino influence on winter–spring precipitation over the southern United States and northern Mexico (from Stahle et al., in press).

The Port Hudson site was revisited and confirmed by Carpenter in 1838 and by the great 19th century geologist, Sir Charles Lyell, in 1846 (Lyell, 1849). Brown and Montz (1986) report a single radiocarbon date of 12,520 ± 410 years for a stump exposed at the site in 1953. However, this date seems unlikely because the deposit is located at the base of a coastal terrace linked stratigraphically to the Eemian interglacial (Delcourt and Delcourt, 1996), some 130,000 years ago.

In a paper read before the Association of Geologists and Naturalists in Boston in 1847, Montroville W. Dickeson described the encroachment of vegetation and infilling of bayous, sloughs, and oxbow lakes in the Mississippi Valley, and the process by which cypress forests become entombed and preserved in sediments (Dickeson and Brown, 1848):

> "Sections of such filled up cypress basins are not infrequently exposed by the changes in the position of the river; they exhibit undisturbed, perfect, and erect cypress stumps, in a series of every elevation with respect to each other, extending from high water mark down to at least twenty-five feet below; measuring out a time when not less than ten fully matured cypress growths must have succeeded each other, the average of whose age could not have been less than four hundred years; thus making an aggregate of four thousand years since the first cypress tree vegetated the basin. There are also instances where prostrate trunks of huge dimensions, are found imbedded in the clay, immediately over which are erect stumps and trees numbering no less than eight hundred concentric layers."

Baldcypress is botanically related to some of the oldest wood remains ever recovered. Among the oldest well-preserved

non-lithified wood ever reported appears to be the Eocene to Oligocene age logs and stumps of *Metasequoia* sp. found on Axel Heiberg Island in the Canadian High Arctic (Jahren and Sternberg, 2002). The *Metasequoia* wood is being exposed at the ground surface by erosion and remains of over 100 trees have been found. The trees apparently grew in a forest that included ancestral *Picea* and *Larix* some 30–50 million years ago, but the *Picea* and *Larix* are not as common or well preserved as *Metasequoia* in the Axel Heiberg deposits. Sixteen large subfossil *Taxodium* stumps were also recently discovered in growth position in 8 million year old deposits in an-open pit lignite mine in Hungary (Alfred Dulai, personal communication, 2007).

Following the Axel Heiberg *Metasequoia* and the Hungarian *Taxodium* wood discoveries, other ancient non-lithified subfossil wood found in quantity includes Kauri in New Zealand (Palmer et al., 2006), subfossil pine in Fennoscandia (Eronen et al., 2002), subfossil oak in Europe and the United States (Leuschner et al., 2002; Stambaugh and Guyette, 2009), and the hundreds of baldcypress stumps and logs buried at several locations on the Atlantic coastal plain of the southeastern United States. These buried baldcypress deposits include upright tree stumps 11 m below street level and 3 m below modern sea level in downtown Philadelphia (Cotter et al., 1993), baldcypress logs, roots and stumps 6 m below street level in Baltimore (Roylance, 1997), and the well-documented Walker Interglacial Swamp buried 6 m below street level in downtown Washington D.C. (Knox, 1966). These three sites are all over 100 km north of the modern range of the species. The Walker Interglacial Swamp is just four blocks north of the White House (Fig. 15), the stumps are up to 2.5 m in diameter, and they were found in separate excavations during the construction of the Mayflower Hotel in 1921, the Operating Engineers Building in 1955, and the National Geographic Building in 1961 (Knox, 1966). The stumps sit upright in growth position in a 3 m thick layer of organic silt and clay with their roots and knees still attached. Knox (1966) provides evidence indicating that the Walker Swamp cypress trees lived during the last super interglacial period (ca 130,000 years ago) when sea level was rising slowly, and that the trees were subsequently drowned and entombed in sediments when sea level rise accelerated and

> "the Potomac River estuary flooded a large portion of what is now downtown Washington, including the site of Walker Swamp and the future site of the White House, and buried the area under silt, sand, and gravel to a depth of 20 feet or more."

If the dating inferences are correct, then this deposit provides *prima facie* evidence for what the future may hold for the low-lying districts of Washington DC in an anthropogenically-warmed world with higher sea levels.

Hollin and Hearty (1990) analyzed Pleistocene sedimentary formations along the Intracoastal Waterway near Myrtle Beach, South Carolina, and differentiated the Waccamaw, Canepatch, and Socastee Formations. The Canepatch Formation includes rooted cypress stumps and fallen logs that were exposed for at least 4 km along the Waterway. They argue that the Canepatch Formation dates to Oxygen Isotope Stage (OIS) 5e, 125,000 to 135,000 years BP (before present), and that the rooted cypress trees were drowned by a Canepatch transgression of sea level to a height some 14–15 m above the modern shoreline (Hollin and Hearty, 1990). Hundreds of large subfossil baldcypress stumps rooted in peaty clay have also been reported at other buried locations along the Southeast coast, including the Williams Pit in Newport News, Virginia (Johnson, 1976), and the Flanner Beach Formation, North Carolina (Mizon, 1986). The magnitude and timing of Pleistocene sea level changes on the Southeast coast remain complex and contentious, but it is possible that some of the buried subfossil cypress deposits in Washington D.C., Newport News, North Carolina, and at Myrtle Beach, South Carolina, date from the same large advance of sea level across the low-lying coastal plain during OIS 5e some 125,000 years ago.

Buried baldcypress wood radiocarbon dated to the Holocene has also been reported (Stahle et al., 1985; Kesel, 2008), and will be needed for significant extension of the calendar-dated chronologies based on living baldcypress trees and surface and submerged logs.

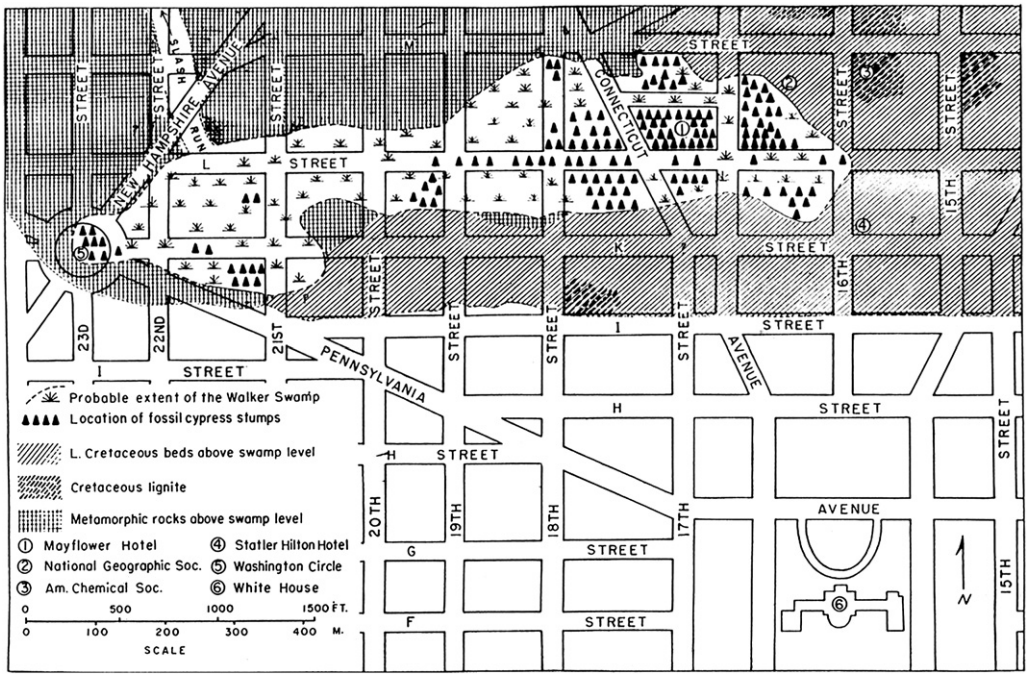


**Fig. 15.** This map locates the sub-surface "Walker Interglacial Swamp" which is buried some 6 m below street level in downtown Washington D.C., only four blocks north of the White House (from Knox, 1966). Large well-preserved baldcypress logs and stumps have been encountered during construction projects, and are believed to have been buried by the Potomac River estuary during warm interglacial conditions and higher sea levels. This deposit has not been absolutely dated, but OIS 5e is a leading hypothesis.

However, to our knowledge no major Holocene age deposits with numerous well-preserved baldcypress logs have yet been reported in the literature. Many small deposits have been noted and a few archaeological sites have produced baldcypress timbers and artifacts (e.g., Pierce, 2010) that may contribute to long chronology development during the Holocene.

## 8. Subfossil baldcypress deposits in South Carolina

Ancient baldcypress logs have been discovered in quantity from buried alluvial deposits in the drainage basin of the Great Pee Dee River, South Carolina. Wood samples from selected logs have been positively identified as *T. distichum* (e.g., Forest Products Laboratory, University of Michigan, 2004; University of Arkansas Tree-Ring Laboratory, 2005). These subfossil baldcypress logs have been recovered from three separate sand quarries on the Lynches and Little Pee Dee River floodplains, approximately 12 m below the modern land surface and include logs from 0.5 to 2.4 m in diameter and up to 30 m in length (Fig. 16). Over 90 logs have already been recovered and hundreds of additional logs are believed to remain buried at all three locations.

The age and origin of these subfossil baldcypress logs are uncertain. The modern land surface is 9 m above sea level and the subfossil logs are found in a white sand unit some 9–12 m below the modern ground surface, implying that the subfossil deposit is at or below modern sea level at all three quarries. The white sand unit is vertically and horizontally confined and appears to meander in the sub-surface somewhat reminiscent of the modern stream channels of the Lynches and Little Pee Dee Rivers (Mr. Ronnie Todd, personal communication, 2004).

High-precision radiocarbon dating was conducted on a selection of 16 subfossil logs from three quarries and all 16 were essentially radiocarbon dead (>40 ka, Table 3). Most of the logs are well preserved in spite of their great antiquity (Fig. 16A). The sapwood appears to have eroded away from most of the Pee Dee subfossil logs we examined (some 50 logs), but many are solid to pith. Many logs still retain the buttress and upper portion of the root system. The cypress logs are completely water saturated when first recovered from the quarry, but when carefully dried they can be sawn, planed, and polished to a lustrous finish suitable for fine woodworking and sculpture. A number of hardwood logs have also been recovered from the same deposit, but they are not as well preserved as the cypress logs.

The buried logs may represent forests that recruited on floodplains crossing exposed continental shelf during a sea level low stand, and might have been subsequently buried by fluvial deposits associated with sea level rise during interglacial conditions (e.g., Baldwin et al., 2006). The white sand layer is overlain by younger sedimentary deposits, some of which also contain subfossil wood, though apparently not in the abundance or quality seen in the white sand unit. However, it is not known if the white sand unit represents a single depositional event or a slow process of accumulation over centuries to millennia. This question has bearing on the absolute contemporaneity of the subfossil logs, and their potential to be used to construct long cross-synchronized annual ring-width chronologies suitable for paleoclimatic analysis. The ideal scenario for dendrochronology might be a gradual time-transgressive channel cut and fill process that generated several successive and overlapping cohorts of contemporaneous trees and logs whose ring patterns can be matched and extended through time for centuries. Preliminary evidence, including the water-sculpted surface of the logs, the lack of sapwood, the fact that none of the buried logs appear to be in growth position, the sub-surface geometry of the white sand unit, and the developmental history of other Coastal

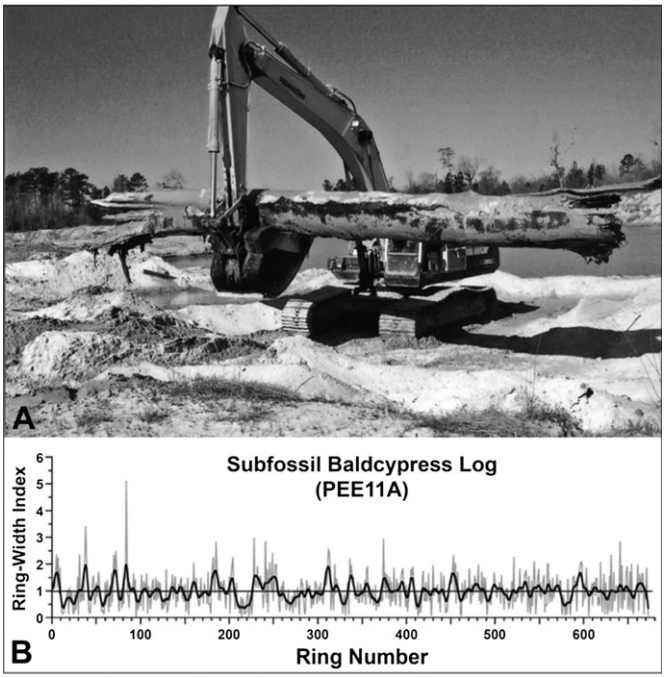


**Fig. 16.** (A) An ancient baldcypress log recovered from 13 m below the modern land surface at a sand quarry on the Little Pee Dee River, Marion County, South Carolina (photograph by Steve Lane). Radiocarbon dating from 16 subfossil cypress logs found in the Little Pee Dee and Lynches River quarries indicates that these deposits are radiocarbon dead (>50 ka; Table 3). (B) The detrended ring-width indices computed for a single subfossil log are plotted (gray), along with a decadal version (black). This log was excavated from the floodplain of the Little Pee Dee River and has 674 annual rings. The absolute dating of this record is not known, but the interannual and decadal variance is similar to the growth of modern baldcypress trees in the Carolinas. Spectral analysis of this series indicates significant concentrations of variance at periods near 2.9, 5.7, 7.9, 17.5, and 52.0 years, which might nominally be linked with ocean-atmospheric forcing from the Pacific and Atlantic. It will be interesting to see if these frequency components also occur in the hundreds of other subfossil logs preserved in these quarries.

**Table 3**
Radiocarbon age determinations for 16 separate subfossil baldcypress (*T. distichum*) logs recovered from buried deposits in three sand quarries on the Little Pee Dee and Lynches Rivers, South Carolina. All determinations were calculated at the Radiocarbon Dating Laboratory, University of Waikato, New Zealand, using a blank of 0.092 ± 0.18% modern, the Libby half-life of 5568 yr with correction for isotopic fractionation. Fifteen logs returned only minimum age determinations, and the single log with a finite age (LYN18, Wk 20761) should also be treated as a minimum age because it is close to the threshold of minimum age assignment and has a low alpha cellulose content (with higher risk for modern contamination; Alan Hogg, personal communication, April 24, 2007).

| Field ID | Lab Number | $\delta^{13}C$ | % Modern (%M ± 1sd) | Age (yr BP) |
|---|---|---|---|---|
| Little Pee Dee River, Marion County, SC, 33.827°N 79.272°W, 6.1 m amsl | | | | |
| PEE03 | Wk 20599 | −20.7 ± −0.2 | −0/1 ± 0.1 | >54,956 BP |
| PEE04 | Wk 20600 | −20.4 ± −0.2 | 0.0 ± 0.1 | >52,408 BP |
| PEE06 | Wk 20601 | −20.9 ± −0.2 | 0.0 ± 0.1 | >53,429 BP |
| PEE10 | Wk 20602 | −21.0 ± −0.2 | 0.0 ± 0.0 | >56,461 BP |
| PEE11A | Wk 20603 | −21.5 ± −0.2 | −0.1 ± 0.1 | >54,128 BP |
| "The Neck," Lynches River, Florence County, SC, 33.845°N 79.520°W, 9.1 m amsl | | | | |
| NEK02 | Wk 20604 | −21.7 ± −0.2 | 0.0 ± 0.1 | >54,905 BP |
| NEK03 | Wk 20605 | −21.7 ± −0.2 | 0.0 ± 0.1 | >53,793 BP |
| NEK05 | Wk 20606 | −20.6 ± −0.2 | 0.0 ± 0.1 | >54,860 BP |
| NEK20 | Wk 20607 | −20.6 ± −0.2 | −0.1 ± 0.1 | >56,376 BP |
| NEK21 | Wk 20608 | −20.7 ± −0.2 | 0.0 ± 0.1 | >54,942 BP |
| Lynches River Quarry, Florence County, SC, 33.989°N 79.819°W, 27.4 m amsl | | | | |
| LYN11 | Wk 20757 | −20.8 ± −0.2 | 0.0 ± 0.1 | >54,996 BP |
| LYN15 | Wk 20758 | −21.1 ± −0.2 | 0.0 ± 0.1 | >49,232 BP |
| LYN16 | Wk 20759 | −22.4 ± −0.2 | 0.0 ± 0.1 | >53,097 BP |
| LYN17 | Wk 20760 | −21.9 ± −0.2 | 0.0 ± 0.1 | >48,639 BP |
| LYN18 | Wk 20761 | −21.1 ± −0.2 | 0.2 ± 0.1 | 51,824 + 4835–2997 BP |
| LYN19 | Wk 20762 | −20.9 ± −0.2 | 0.0 ± 0.1 | >54,278 BP |

Plain alluvial deposits may favor this time-transgressive cut and fill model.

Episodic extreme flood events might also explain the subfossil cypress deposits, with little or no temporal overlap between the trees entombed in each successive event. Other depositional scenarios can also be imagined, including a transgression of sea level as postulated for the mid-Pleistocene age subfossil deposits elsewhere on the Atlantic Coastal Plain (Knox, 1966; Hollin and Hearty, 1990).

We have examined several polished baldcypress specimens already recovered from the sand quarries and identified from 100 to 700 annual growth rings (e.g., Fig. 16B). Given the large number of subfossil cypress logs recovered from the sand quarries and the significant number of annual growth rings found on some individual logs, there may be potential to develop exactly crossdated tree-ring chronologies from logs of contemporaneous age at each sand quarry. If successful, these tree-ring chronologies would "float" in time, where exact calendar year dating would only be approximated based on some other independent dating method (e.g., stratigraphic position, optically-stimulated luminescence). Nevertheless, exactly crossdated and well-replicated floating chronologies of several hundred to several thousand years in length from the Carolinas could be valuable for the analysis of climate variability during the period when the trees grew and were subsequently entombed.

## 9. Conclusions

Baldcypress trees have been used to develop a network of centuries to millennium-long tree-ring chronologies for the southeastern United States, Mexico, and western Guatemala. These chronologies invariably respond to the growing season moisture balance and are positively correlated with precipitation in spite of frequently flooded site conditions. Separate chronologies of earlywood and latewood width have been developed at many baldcypress sites and can be used for the reconstruction of both spring and summer precipitation. These spring and summer precipitation reconstructions provide a more complete picture of growing season climate and exhibit a very different response to forcing from El Nino conditions in the tropical Pacific. Not all of these chronologies are over 1000-years long, but most could be improved and extended deeper into prehistory with additional collections of old living trees, construction timbers from historic buildings, and especially with relict surface and buried subfossil wood. Because old non-commercial baldcypress trees survive at many locations across the southeastern United States and Mexico, there is good potential to improve the density and spatial distribution of the cypress chronology network and the derived paleoclimatic reconstructions.

Thirty-six Montezuma baldcypress chronologies have been developed thus far for Mexico and Guatemala, but just 10 date before AD 1500. The oldest Montezuma baldcypress have been found in a mildly saline wetland at Los Peroles, San Luis Potosi, where the two oldest individuals are at least 1500-years old, and on magnesium-rich basalt terrain in Barranca de Amealco, Queretaro, where several trees are over 1000-years old and the oldest dated ring begins in AD 771. The unique environmental conditions at these two old-growth sites suggest that soil or water chemistry may be important in the advanced longevity of the species. Soil chemistry, particularly magnesium-rich soils, have been previously associated with longevity in trees for several species. If physical explanations can be found for the longevity of Montezuma baldcypress, then it might be possible to focus the search for the oldest trees in the remote and highly complex terrain of Mexico.

The buried subfossil cypress logs recovered from South Carolina demonstrate the durability of the wood and indicate the potential for subfossil cypress recovery at other locations in the South. Other deposits of buried cypress logs have been reported in the literature, including well-preserved logs dating to the early, middle, and late-Holocene (Stahle et al., 1985), and to earlier glacial and interglacial periods (some estimated to be over 100,000 years old; Knox, 1966; Brown and Montz, 1986; Hollin and Hearty, 1990; Delcourt and Delcourt, 1996). None of these other reported subfossil baldcypress deposits are known to contain such abundant and well-preserved logs as found in the South Carolina quarries, but they nevertheless indicate some potential, however remote, to eventually compile an unbroken, perfectly dated annual ring-width chronology for the Atlantic or Gulf Coastal Plain dating back well into the Holocene, and on a discontinuous floating chronology basis into the late Pleistocene.

## Acknowledgments

We thank E.R. Cook for advice and assistance with the Kalman Filter; Rodolfo Acuna, Matt Therrell, Yovany Diaz, Oscar Chavez, Steve Lane, Ricky Cox, and Larry Benson for field assistance, and Keith Newton for photography. Funded by the National Science Foundation Paleoclimatology Program (ATM-0400713, and ATM-0753399), the National Oceanic and Atmospheric Administration, CCDD (NA08OAR4310727), and the Graduate School of the University of Arkansas, Fayetteville.

## References

Allen, J.A., Chambers, J.L., McKinney, D., 1994. Intraspecific variation in the response of *Taxodium distichum* seedlings to salinity. Forest Ecology and Management 70, 203–214.

Baldwin, W.E., Morton, R.A., Putney, T.R., Katuna, M.P., Harris, M.S., Gayes, P.T., Driscoll, N.W., Denny, J.F., Schwab, W.C., 2006. Migration of the Pee Dee River system inferred from ancestral paleochannels underlying the South Carolina Grand Strand and Long Bay inner shelf. GSA Bulletin 118, 533–549.

Bartram, W., 1791. The Travels through North & South Carlina, Georgia, East & West Florida, the Cherokee Country, the Extensive Territories of the Muscogulges, or Creek Confederacy, and the Country of the Choctaws. Penguin Books, New York, NY (1988).

Briffa, K.R., Melvin, T., 2011. A closer look at regional curve standardization of tree-ring records: justification of the need, a warning of some pitfalls, and suggested improvements in its application. In: Hughes, M.K., Swetnam, T.W., Diaz, H.F. (Eds.), Dendroclimatology. Springer, Dordrecht.

Brown, C.A., Montz, G., 1986. Baldcypress: The Tree Unique, the Wood Eternal. Claitor's Publishng Division, Baton Rouge, Louisiana.

Cobb, K., Charles, C.D., Cheng, H., Edwards, R.L., 2003. El Nino-Southern Oscillation and tropical Pacific climate during the last millennium. Nature 424, 271–276.

Conner, W.H., Inabinette, W., 2005. Identification of salt tolerant baldcypress (*Taxodium distichum* (L.) Rich) for planting in coastal areas. New Forests 29, 305–312.

Cook, E.R., 1985. A Time Series Analysis Approach to Tree-Ring Standardization. Dissertation. University of Arizona, Tucson.

Cook, E.R., Peters, K., 1981. The smoothing spline: a new approach standardizing forest interior tree-ring series for dendroclimatic studies. Tree Ring Bulletin 41, 45–53.

Cook, E.R., Briffa, K.R., Meko, D.M., Graybill, D.A., Funkhouser, G., 1995. The 'segment length curse' in long tree-ring chronology development for paleoclimatic studies. The Holocene 5, 229–237.

Cook, E.R., Meko, D.M., Stahle, D.W., Cleaveland, M.K., 1999. Drought reconstructions for the continental United States. Journal of Climate 12, 1145–1162.

Cook, E.R., Seager, R., Cane, M.A., Stahle, D.W., 2007. North American Drought: reconstructions, causes, and consequences. Earth Science Reviews 81, 93–134.

Cotter, J.L., Roberts, D.G., Parrington, M., 1993. The Buried Past, an Archaeological History of Philadelphia. University of Pennsylvania Press, Philadelphia.

Davidson, G.R., Laine, B.C., Galicki, S.J., Threlkeld, S.T., 2006. Root zone hydrology: why bald cypress in flooded wetlands grow more when it rains. Tree-Ring Research 62, 3–12.

Delcourt, P.A., Delcourt, H.R., 1996. Quaternary paleoecology of the Lower Mississippi Valley. Engineering Geology 45, 219–242.

Dennis, J.V., 1988. The Great Cypress Swamps. Louisiana State University, Baton Rouge.

Dickeson, M.W., Brown, A., 1848. On the cypress timber of Mississippi and Louisiana. American Journal of Science and Arts 5, 515–522.

Douglass, A.E., 1920. Evidence of climatic effects in the annual rings of trees. Ecology 1, 24–32.

Early, L.S., 1990. Clues from the Methuselahs. Audubon 92, 68–74.

Eronen, M., Zetterberg, P., Briffa, K.R., Lindholm, M., Merilainen, J., Timonen, M., 2002. The supra-long Scots pine tree-ring record for Finnish Lapland: part 1, chronology construction and initial inferences. Holocene 12, 673–680.

Ewel, K.C., Odum,, H.T. (Eds.), 1984. Cypress Swamps. University of Florida Press, Gainesville, 472 pp.

Folland, C.K., Karl, T.R., 2001. Observed climate variability and change. In: Houghton,, J.T., et al. (Eds.), Climate Change 2001 : The Scientific Basis. Contribution of Working Group I to the Third Assessment Report of the Intergovernmental Panel on Climate Change. Cambridge University Press, Cambridge, United Kingdom and New York, NY, USA.
Fritts, H.C., 2001. Tree Rings and Climate. Blackburn Press, New Jersey.
Hollin, J.T., Hearty, P.J., 1990. South Carolina interglacial sites and Stage 5 sea levels. Quaternary Research 33, 1–17.
Jahren, A.H., Sternberg, L.S.L., 2002. Eocene meridional weather patterns reflected in the oxygen isotopes of Arctic fossil wood. GSA Today 12, 4–9.
Johnson, G.H., 1976. Geology of the Mulberry Island, Newport News North, and Hampton Quadrangles, Virginia. Report of Investigations 41. Virginia Division of Mineral Resources, Charlottesville, VA.
Kaplan, A., Cane, M.A., Kushnir, Y., Clement, A.C., Blumenthal, M.B., Rajagopalan, B., 1997. Analyses of global sea surface temperature 1856–1991. Journal of Geophysical Reseach 102, 27835–27860. Update to 2005. http://www.cdc.noaa.gov/cdc/data.kaplan_sst.
Kesel, R.H., 2008. A revised Holocene geochronology for the Lower Mississippi Valley. Geomorphology 101, 78–89.
King, W., Cahalane, V.H., 1939. A Cypress Swamp National Monument. Internal Report of the Wildlife Division. National Park Service, Washington, D.C.
Knox, A.S., 1966. The Walker interglacial swamp, Washington D.C. Journal of the Washington Academy of Sciences 56, 1–8.
Kurz, H., Demaree, D., 1934. Cypress buttresses and knees in relation to water and air. Ecology 15, 36–41.
Leuschner, H.H., Sass-Klaassen, U., Jansma, E., Baillie, M.G.L., Spurk, M., 2002. Subfossil European bog oaks: population dynamics and long-term growth depressions as indicators of changes in the Holocene hydro-regime and climate. The Holocene 12, 695–706.
Little Jr., E.L., 1971. Atlas of United States Trees. In: Conifers and Important Hardwoods, vol. 1 U.S.D.A. Miscellaneous Publication 1146.
Lyell, C., 1849. A Second Visit to the United States of North America, vol. II. John Murray, Albemarle Street, London.
Mann, M.E., Bradley, R.S., Hughes, M.K., 2000. Long-term variability in the El Nino Southern Oscillation and associated teleconnections. In: Diaz, H.F., Markgraf, V. (Eds.), El Nino and the Southern Oscillation: Multiscale Variability and Its Impacts on Natural Ecosystems and Society. Cambridge University Press, Cambridge, UK, pp. 357–412.
Martinez, M., 1963. Las Pinaceas Mexicanas. Universidad Autonoma de Mexico, Cuidad Universitaria, Mexico D.F.
Mattoon, W.R., 1915. The Southern Cypress. In: USDA Bulletin No. 272 Washington, D.C.
McGregor, S., Timmermann, A., Timm, O., 2010. A unified proxy for ENSO and PDO variability since 1650. Climate of the Past 6, 1–17.
Meko, D.M., Baisan, C.H., 2001. Summer rainfall from latewood width. International Journal of Climatology 21, 697–708.
Mizon, R.B., 1986. Depositional Environments and Paleogeography of the Interglacial Flanner Beach Formation, Cape Lookout Area, North Carolina. In: Geological Society of America Centennial Field Guide-Southeastern Section, 315–320 pp.
National Audubon Society, 1985. The Francis Beidler Forest (A National Audubon Society Wildlife Sanctuary).
Palmer, J., Lorrey, A., Turney, C.S.M., Hogg, A., Baillie, M., Fifield, K., Ogden, J., 2006. Extension of New Zealand kauri (*Agathis australis*) tree-ring chronologies into Oxygen Isotope Stage (OIS)-3. Journal of Quaternary Science 21, 779–787.
Philander, G.S., 1990. El Nino, La Nina, and the Southern Oscillation. Academic Press, New York, 289 pp.
Pierce, G., 2010. Synthesis of the Prehistoric Archaeological Investigations of Lake Phelps, Washington County, North Carolina. MA Thesis, East Carolina University, Greenville, NC.
Rayner, N.A., Parker, D.E., Horton, E.B., Folland, C.K., Alexander, L.V., Rowell, D.P., Kent, E.C., Kaplan, A., 2003. Global analyses of sea surface temperature, sea ice, and night marine air temperature since the late nineteenth century. Journal of Geophysical Research 108 (D14), 4407. doi:10.1029/2002JD002670.
Roylance, F.D., March 25 1997. Unearthing roots of time before fans stadium: a grove of bald cypress trees that may be up to 10 million years old was discovered while building the home of the Ravens. The Baltimore Sun.
Seager, R., Tzanova, A., Nakamura, J., 2009. Drought in the southeastern United States: causes, variability over the last millennium, and the potential for future hydroclimatic change. Journal of Climate 22, 5021–5045.
Soltis, P.S., Soltis, D.E., Smiley, C.J., 1992. An *rbcL* sequence from a Miocene *Taxodium* (bald cypress). Proceedings of the National Academy of Science 89, 449–451.
Stahle, D.W., Cleaveland, M.K., 1992. Reconstruction and analysis of spring rainfall over the Southeastern U.S. for the past 1000 years. Bulletin of the American Meteorological Society 73, 1947–1961.
Stahle, D.W., Cook, E.R., White, J.W.C., 1985. Tree-ring dating of baldcypress and the potential for millennia-long chronologies in the Southeast. American Antiquity 50, 796–802.
Stahle, D.W., Cleaveland, M.K., Hehr, J.G., 1988. North Carolina climate changes reconstructed from tree rings: A.D. 372–1985. Science 240, 1517–1519.
Stahle, D.W., Van Arsdale, R., Cleaveland, M.K., 1992. Tectonic signal in baldcypress trees at Reelfoot Lake, Tennessee. Seismological Research Letters 63, 439–448.
Stahle, D.W., Cleaveland, M.K., Blanton, D.B., Therrell, M.D., Gay, D.A., 1998. The lost colony and Jamestown droughts. Science 280, 564–567.
Stahle, D.W., Cleaveland, M.K., Griffin, R.D., Spond, M.D., Fye, F.K., Culpepper, R.B., Patton, D., 2006. Decadal drought effects on endangered woodpecker habitat. Eos, Transactions of the American Geophysical Union 87, 121–125.
Stahle, D.W., Cleaveland, M.K., Grissino-Mayer, H., Griffin, R.D., Fye, F.K., Therrell, M.D., Burnette, D.J., Meko, D.M., Villanueva Diaz, J., 2009. Cool and warm season precipitation reconstructions over western New Mexico. Journal of Climate 22, 3729–3750.
Stahle, D.W., Villanueva Diaz, J., Burnette, D.J., Cerano Paredes, J., Heim Jr., R.R., Fye, F.K., Acuna Soto, R., Therrell, M.D., Cleaveland, M.K., Stahle, D.K., 2011a. Major Mesoamerican droughts of the past millennium. Geophysical Research Letters 38, L05703. doi:10.1029/2010GL046472.
Stahle, D.W., Burnette, D.J., Villanueva Diaz, J., Heim, Jr., R.R., Fye, F.K., Cerano Paredes, J., Acuna Soto, R., Cleaveland, M.K., Pacific and Atlantic influences on Mesoamerican climate over the past millennium. Climate Dynamics, in press.
Stahle, D.W., Wolfe, K., Griffin, R.D., 2011b. Visiting the ancient baldcypress trees on the Black River. Afield, the North Carolina Chapter of the Nature Conservancy, Fall 2011, 6 p.
Stambaugh, M.C., Guyette, R.P., 2009. Progress in constructing a long oak chronology from the central United States. Tree-Ring Research 65, 147–156.
Stokes, M.A., Smiley, T.L., 1996. An Introduction to Tree-Ring Dating. University of Arizona Press, Tucson.
Thomas, B.A., Spicer, R.A., 1987. The Evolution and Paleobiology of Land Plants. Croom Helm, London.
Villanueva-Diaz, J., Stahle, D.W., Luckman, B.H., Ceranno-Paredes, J., Therrell, M.D., Moran Martinez, R., Cleaveland, M.K., 2007. Potenical dendrocronologico de *Taxodium mucronatum* Ten. y acciones para su conservacion en Mexico. Ciencia Forestal en Mexico 32 (101), 9–38.
Visser, H., Molenaar, J., 1988. Kalman filter analysis in dendroclimatology. Biometrics 44, 929–940.
Wharton, C.H., Kitchens, W.M., Sipe, T.W., 1982. The Ecology of Bottomland Hardwood Swamps of the Southeast: A Community Profile. U.S. Fish and Wildlife Service, Washington, D.C. FWS/OBS-81/37.
Yanosky, T.M., Hupp, C.R., Courtney, C.T., 1995. Chloride concentrations in growth rings of *Taxodium distichum* in a saltwater-intruded estuary. Ecological Applications 5, 785–792.